Journal of Paleontology, 96(3), 2022, p. 638–657

0022-3360/22/1937-2337
doi: 10.1017/jpa.2021.108

JOURNAL OF PALEONTOLOGY
A PUBLICATION OF THE Paleontological SOCIETY

Lochkovian (Lower Devonian) conodonts from the Alengchu section, western Yunnan, China

Jian-Feng Lu,[1]* Xue-Ping Ma,[2] Wen-Kun Qie,[1] Kun Liang,[1] and Bo Chen[1]

[1]Nanjing Institute of Geology and Palaeontology and Center for Excellence in Life and Paleoenvironment, Chinese Academy of Sciences, East Beijing Road 39, Nanjing 210008, China <jflu@nigpas.ac.cn>, <wkqie@nigpas.ac.cn>, <kliang@nigpas.ac.cn>, <chenbo@nigpas.ac.cn>
[2]The Key Laboratory of Orogenic Belts and Crustal Evolution (MOE), School of Earth and Space Sciences, Peking University, Yiheyuan Road 5, Beijing 100871, China <maxp@pku.edu.cn>

Abstract.—The Lochkovian (Lower Devonian) conodont biostratigraphy in China is poorly known, and conodont-based subdivision schemes for the Lochkovian in peri-Gondwana (the Spanish Central Pyrenees, the Prague Synform, Sardinia, and the Carnic Alps) have not been tested in China. Therefore, we studied conodonts from the lower part (Bed 9 to Bed 13) of the Shanjiang Formation at the Alengchu section of Lijiang, western Yunnan to test the application of established subdivision schemes. The conodont fauna is assignable to 12 taxa belonging to eight genera (*Ancyrodelloides*, *Flajsella*, *Lanea*, *Wurmiella*, *Zieglerodina*, *Caudicriodus*, *Pelekysgnathus*, and *Pseudooneotodus*), and enables recognition of two chronostratigraphical intervals from the lower part of the Shanjiang Formation. The interval ranging from the uppermost part of Bed 9 to the upper part of Bed 10 belongs to the lower Lochkovian; whereas an interval covering the uppermost part of Bed 11 to the upper part of Bed 13 is correlated with the upper half of the middle Lochkovian. The Silurian-Devonian boundary is probably located within Bed 9, in the basal part of the Shanjiang Formation. However, the scarcity of specimens precludes definitive identification of bases of the lower, middle, and upper Lochkovian as well as other conodont zones recognized in peri-Gondwana.

Introduction

The conodont-based Lochkovian (Lower Devonian) subdivision has been extensively investigated by worldwide Devonian conodont researchers. The first comprehensive subdivision scheme was presented by Klapper (1977), who subdivided the Lochkovian in western North America into the *hesperius* Zone, *eurekaensis* Zone, which already was defined by Klapper and Murphy (1975), *Ozarkodina* n. sp. D Zone (= *delta* Zone), and *pesavis* Zone, which already was defined by Fåhræus (1971). However, great difficulty was encountered in the application of this central Nevada scheme to the Lochkovian in other places around the world, as suggested by Valenzuela-Ríos (1994a, b) and Valenzuela-Ríos and Murphy (1997). On the basis of the comparison of conodont records from the Spanish Central Pyrenees with those from central Nevada, Valenzuela-Ríos (1994a) subdivided the *delta* and *pesavis* zones into five and two zones, respectively. Later, Valenzuela-Ríos (1994b) discussed the different uses of the *pesavis* Zone and proposed a new subdivision of this Zone and the uppermost part of the *delta* Zone into the *pandora* β-*gilberti* and *gilberti-eosulcatus* zones. Valenzuela-Ríos and Murphy (1997) subdivided the Lochkovian into the lower, middle, and upper parts based upon the evolution and global records of the genus *Ancyrodelloides* Bischoff and Sannemann, 1958. The lower boundaries of the middle and upper Lochkovian were suggested to be defined by the first occurrences of *Lanea omoalpha* Murphy and Valenzuela-Ríos, 1999, and *Masarella pandora* Murphy et al., 1981 β morphotype, respectively. The middle Lochkovian consists, in ascending order, of the *omus* α-*eleanorae*, *eleanorae-trigonicus*, and *trigonicus-pandora* β zones. Subsequently, the *omus* α-*eleanorae* Zone was further subdivided into the *omoalpha-transitans* and *transitans-eleanorae* zones (Murphy and Valenzuela-Ríos, 1999). Another alternative zonal scheme proposed by Slavík et al. (2012) in the Prague Synform was similar to that of Murphy and Valenzuela-Ríos (1999) in the upper half of the middle Lochkovian and upper Lochkovian zonation, but the lower Lochkovian and lower half of the middle Lochkovian zonation consists, in ascending order, of the *hesperius-optima*, *optima-breviramus*, *breviramus-omoalpha*, *omoalpha-carlsi*, *carlsi-eoeleanorae*, *eoeleanorae-boucoti*, and *boucoti-transitans* zones. In addition, they shifted the position of the lower boundary of the middle Lochkovian to the entry of *A. carlsi* (Boersma, 1973) (= *Lanea carlsi* in their paper). Meanwhile, Corradini and Corriga (2012) proposed a Lochkovian zonation for Sardinia and the Carnic Alps that differs from those in the Spanish Central Pyrenees and the Prague Synform in that the lower Lochkovian and lower half of the middle Lochkovian are subdivided into the *hesperius* and *carlsi* zones. By comparing records from the Spanish Central Pyrenees with those from the Prague Synform, Valenzuela-Ríos et al. (2015) subdivided the former *trigonicus-pandora* β Zone into the *trigonicus-kutscheri* and *kutscheri-pandora* β zones. The recommended standard Lochkovian conodont zonation is mainly established on the basis of these peri-Gondwana subdivision schemes (Becker et al., 2020).

The Lochkovian zonation of Klapper (1977) was widely applied in China (C.Y. Wang, 1981, 1982; Li, 1987; Wang

*Corresponding author

and Zhang, 1988; Liao and Xia, 1996; Xia, 1997; Wang et al., 2001; P. Wang, 2006), despite the subsequent recognition that this scheme is not globally applicable (Valenzuela-Ríos and Murphy, 1997). Accordingly, it is clear that these previously reported Lochkovian conodont zonations in China cannot be precisely correlated with those in the Spanish Central Pyrenees, central Nevada, the Prague Synform, Sardinia, and the Carnic Alps. It should be noted that the strata in most of the studied Lochkovian sections in China are discontinuous or poorly exposed, resulting in only one to two zones of Klapper (1977) being reported from one section in most cases. Furthermore, all of the sections located in remote or mountainous areas do not belong to the South China Block, but to other blocks or terranes. According to Lu and Chen (2016), the widely distributed and extensively developed Devonian carbonate succession in the South China Block started in the early Emsian, while the Lochkovian is mainly represented by sandstone, siltstone, and mudstone. Recently, Wang et al. (2018) studied the Lower Devonian conodont biostratigraphy at the well-known Alengchu section (western Yunnan), but only a few Lochkovian taxa, without important and unequivocal zonal markers, were collected, thus precluding a precise and high-resolution conodont-based subdivision. This locality probably represents one of the few places where the Lower Devonian carbonate succession is continuously developed. Therefore, the goal of this research is to update the Lochkovian conodont biostratigraphy at the Alengchu section, which will furnish important Chinese materials for intercontinental correlation, and to test the global relevance of peri-Gondwana conodont-based subdivision schemes in China.

Geological setting

The Alengchu section is named after a small village, Alengchu, along the Jinshajiang River that is situated ~50 km northeast of Lijiang, western Yunnan (Fig. 1). The Lijiang area, plus the adjacent Yanbian or Panzhihua area (southern Sichuan), the geographically so-called Yanbian-Lijiang or Panzhihua-Lijiang district, was usually thought by tectonic geologists to constitute the southwestern margin of the South China Block (Zhang et al., 2013). However, mainly based on the comparison of the Silurian conodonts, brachiopods, and graptolites between the Panzhihua-Lijiang district and the South China Block, Rong et al. (2003) suggested that this district is not a southwestern component of the South China Block. Later, in a study of the Silurian conodont biostratigraphy at the Baizitian section, Panzhihua, Wang et al. (2009) proposed another hypothesis that the Panzhihua-Lijiang district probably belongs to neither the South China Block nor the Lhasa Block, but to an unknown small terrane. This opinion on the provenance of the Panzhihua-Lijiang district was recently further supported by Wang et al. (2016), who noted the great differences in the tectono-geographical location, stratigraphic sequence, sedimentary development, and faunal composition among the Panzhihua-Lijiang district, the South China Block, and the Lhasa Block.

The Lower Devonian is continuously developed and well exposed at the Alengchu section. Yu and Liao (1978) first subdivided the Lower Devonian in ascending order into the Shanjiang, Alengchu, and Banmandaodi formations. For the

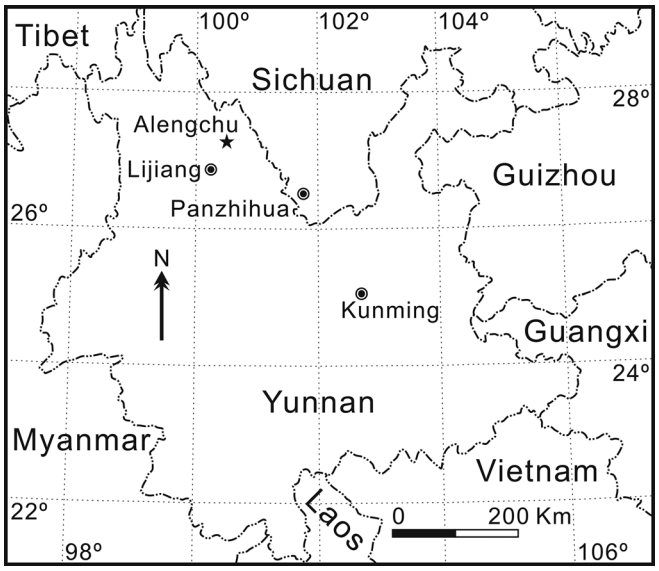

Figure 1. Location of the study area, with the star showing the site of the Alengchu section in western Yunnan, China.

underlying Silurian part, two lithological units, consisting in ascending order of the Longmaxi and Baizitian formations, was adopted by Wang et al. (2018). The Silurian Baizitian Formation, which is marked by thick-bedded nodular limestone, is conformably overlain by the Devonian Shanjiang Formation, which is composed of thin- to medium-bedded bioclastic limestone intercalated with siltstone and shale. The Alengchu Formation is represented by medium- to thick-bedded limestone intercalated with shale. The overlying Banmandaodi Formation consists mainly of sandstone, shale, and limestone. Benthic and pelagic fossils, including rugose corals, tentaculites, and conodonts, are abundant throughout the whole succession of this section. By subdividing the Lower Devonian rugose corals at the Alengchu section into five assemblages, Yu and Liao (1978) pointed out that the rugose coral fauna in Lijiang shows a great difference from the contemporaneous rugose coral fauna in the South China Block. Subsequently, the Lower Devonian tentaculites from the Shanjiang Formation and lower part of the Alengchu Formation were studied by Jiang (1980). Wang (1982) was the first to briefly report the conodont fauna from the Shanjiang Formation to the Banmandaodi Formation and made a preliminary determination on the ages of these lithological units. Recently, Wang et al. (2018) re-studied this section and demonstrated that the Shanjiang Formation can be correlated with the Lochkovian and Pragian, whereas the Alengchu Formation belongs to the lower part of the Emsian.

Materials and methods

Twenty-four limestone samples, each weighing 3–4 kg, were collected in 2019 from the uppermost part of the Baizitian Formation to the lower part of the Shanjiang Formation at the Alengchu section (Table 1; Fig. 2). The samples were crushed mechanically into small pieces of ~2–5 cm in diameter and dissolved in dilute (8–12%) acetic acid. The insoluble residues were then washed, air-dried, and finally concentrated by

https://doi.org/10.1017/jpa.2021.108 Published online by Cambridge University Press

Table 1. Occurrence of conodont taxa from the lower part of the Shanjiang Formation at the Alengchu section.

Sample no. (ALC)	9-4m	9-10m	10-2m	10-6m	10-10m	10-15m	10-19m	10-23m	11-3m	11-9m	12-6m	12-10m	13-13m	13-16m	Total number
Wurmiella excavata (Pa)	1						3	4							8
Caudicriodus sp. B (I)		5	2	4	1		1	2							15
Zieglerodina planilingua (Pa)		1		1				5							7
Zieglerodina remscheidensis (Pa)			2			2	2	5							11
Pseudoneotodus beckmanni					1		2	2							5
Zieglerodina eladioi (Pa)						1	2	4							7
Wurmiella tuma (Pa)										1	1+1 aff.		2		4+1 aff.
Lanea omoalpha (Pa)									1						1
Ancyrodelloides transitans (Pa)											1				1
Lanea telleri (Pa)												1			1
(Pb)												1			1
Flajsella stygia (Pa)												1			1
Pelekysgnathus sp. (I)														1	1
Total number	1	6	4	5	2	3	10	22	1	1	3	3	2	1	64

heavy-liquid separation using sodium polytungstate. Specimens coated with gold were photographed using a Scanning Electron Microscope (SEM) in the Nanjing Institute of Geology and Palaeontology, Chinese Academy of Sciences.

Repository and institutional abbreviation.—All specimens described and illustrated herein are deposited in the collections of the Nanjing Institute of Geology and Palaeontology (NIGP), Chinese Academy of Sciences.

Systematic paleontology

Nomenclature of the Pa and I elements proposed by Murphy and Valenzuela-Ríos (1999, text-fig. 2) and Murphy (2016, fig. 1), respectively, is followed herein.

Order Ozarkodina Dzik, 1976
Family Spathognathodontidea Hass, 1959
Genus *Ancyrodelloides* Bischoff and Sannemann, 1958

Type species.—*Ancyrodelloides trigonica* Bischoff and Sannemann, 1958.

Ancyrodelloides transitans (Bischoff and Sannemann, 1958)
Figure 3.1, 3.2

1958 *Spathognathodus transitans* Bischoff and Sannemann, p. 107, pl. 13, figs. 4, 5, 12, 14.
1978 *Spathognathodus transitans* Bischoff and Sannemann; Serpagli et al., pl. 27, fig. 5.
1979 *Ozarkodina transitans* (Bischoff and Sannemann); Lane and Ormiston, p. 58, pl. 1, fig. 41, pl. 2, figs. 4, 5, 8, 9, 12, 13, pl. 3, fig. 21.
1980 *Ozarkodina transitans* (Bischoff and Sannemann); Klapper and Johnson, p. 450.
1985a *Ozarkodina transitans* (Bischoff and Sannemann); Mastandrea, p. 255, pl. 2, fig. 2, pl. 5, figs. 14, 15, 17–19.
1985 *Ancyrodelloides transitans* (Bischoff and Sannemann); Schönlaub, pl. 2, figs. 22, 24, pl. 3, fig. 1.
1986 *Ancyrodelloides transitans* (Bischoff and Sannemann); Barca et al., pl. 31, fig. 6.
1988 *Ancyrodelloides transitans* (Bischoff and Sannemann); Wang and Zhang, pl. 1, fig. 11.
1989 *Ancyrodelloides transitans* (Bischoff and Sannemann) beta morph Lane and Ormiston; Wilson, p. 137, pl. 12, figs. 18, 19.
1991 *Ancyrodelloides transitans* (Bischoff and Sannemann); Ziegler, p. 25, pl. 1, fig. 4.
1992 *Cruciodus transitans* (Bischoff and Sannemann); Bardashev and Ziegler, pl. 2, figs. 14, 15, 19, 25.
1992 *Ancyrodelloides transitans* (Bischoff and Sannemann); Barrick and Klapper, p. 48, pl. 4, fig. 13, pl. 5, figs. 1–5.
1994a *Ancyrodelloides transitans* (Bischoff and Sannemann); Valenzuela-Ríos, p. 41, pl.1, figs. 11, 14–18, 20, pl. 2, figs. 2, 4, 5, 8, 16. [with synonymy list]
1998 *Ancyrodelloides transitans* (Bischoff and Sannemann); Lazreq and Ouanaimi, pl. 1, figs. 10, 11, 13.
1998 *Ancyrodelloides transitans* (Bischoff and Sannemann); Slavík, p. 159, pl. 1, figs. 3, 4.
1998 *Ancyrodelloides transitans* (Bischoff and Sannemann); Valenzuela-Ríos and García-López, pl. 1, figs. 6, 8–10.
?2001 *Ancyrodelloides transitans* (Bischoff and Sannemann); Corradini et al., pl. 1, fig. 3.
2003 *Ancyrodelloides transitans* (Bischoff and Sannemann) alpha morphotype Lane and Ormiston; Farrell, p. 132, pl. 5, figs. 10–12.
non 2006 *Ancyrodelloides transitans* (Bischoff and Sannemann); Wang, p. 213, pl. 3, figs. 10–12.

https://doi.org/10.1017/jpa.2021.108 Published online by Cambridge University Press

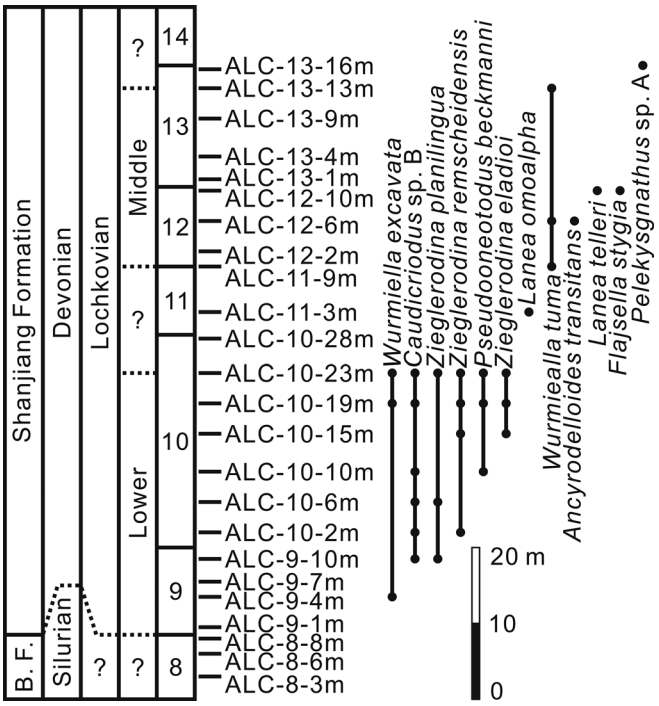

Figure 2. Distribution of conodonts in the lower part (Bed 9 to Bed 13) of the Shanjiang Formation at the Alengchu section, Lijiang, western Yunnan. Abbreviation: B.F., Baizitian Formation.

2007 *Ancyrodelloides transitans* (Bischoff and Sannemann); Jansen et al., fig. 3.9, 3.10.
2007 *Ancyrodelloides transitans* (Bischoff and Sannemann); Suttner, p. 29, pl. 21, figs. 3, 6–9.
2012 *Ancyrodelloides transitans* (Bischoff and Sannemann); Corradini and Corriga, fig. 6N.
2012 *Ancyrodelloides transitans* (Bischoff and Sannemann); Slavík et al., fig. 6.10.
2013 *Ancyrodelloides transitans* (Bischoff and Sannemann); Mavrinskaya and Slavík, fig. 5S, T.
2014b *Ancyrodelloides transitans* (Bischoff and Sannemann); Corriga et al., fig. 5X.
2016 *Ancyrodelloides transitans* (Bischoff and Sannemann); Corradini et al., pl. 4, fig. 11.
2017 *Ancyrodelloides transitans* (Bischoff and Sannemann); Schönlaub et al., pl. 3, fig. 14.
2017 *Ancyrodelloides transitans* (Bischoff and Sannemann); Slavík, fig. 6.10.
2017 *Ancyrodelloides transitans* (Bischoff and Sannemann); Valenzuela-Ríos and Liao, fig. 4.7, 4.8.
2017a *Ancyrodelloides transitans* (Bischoff and Sannemann); Valenzuela-Ríos et al., fig. 6.1.
2017b *Ancyrodelloides transitans* (Bischoff and Sannemann); Valenzuela-Ríos et al., fig. 4.4.

Holotype.—BiSa 1958/26 from the Transgressionshorizont at Schübelebene near Elbersreuth, Frankenwald, Germany (Bischoff and Sannemann, 1958, pl. 13, fig. 5).

Description.—The anterior process is broken, with the two posteriormost oval and pointed denticles preserved. The posterior process is arched downwards posteriorly, slightly deflected inwards, and consists of four stout denticles and one tiny denticle with an oval cross-section, descending in height towards the posterior end and connected by a thin ridge. The platform on the posterior process is poorly developed and bench-like shaped, while it is almost undeveloped on the remnant of the anterior process. The outer process is twice as long as the inner process. Both processes meet the longitudinal axis of the unit at an angle of ~90°. The inner process has a rounded termination and bears only one thick denticle that has an oval cross-section, whereas the outer process has two stout denticles. A thin ridge extends from the tip of the denticle on the inner process via the cusp to the two denticles on the outer process. The platform on the inner and outer processes is poorly developed and narrow. Being only slightly higher than adjacent denticles on the anterior and posterior processes, the cusp is not prominent and almost the same size as the denticles on the inner and outer processes. On the lower side, the shallow and medium-sized basal cavity expands beneath the lateral processes and almost reaches the slightly pointed terminations on both the inner and outer sides. The basal cavity continues posteriorly as a narrow groove that runs to the distal end of the unit.

Material.—One specimen from sample ALC-12-6m.

Remarks.—Murphy and Matti (1983, p. 21, text-fig. 5) pointed out the great difference in the shape of lateral terminations of the basal cavity between *A. trigonicus* Bischoff and Sannemann, 1958, and *A. transitans*. *Ancyrodelloides trigonicus* has a small pit beneath the cusp that tapers to a point laterally for a short distance; in contrast, *A. transitans* has a shallow or moderately deep basal cavity that is bluntly rounded laterally and may reach the terminations of lateral processes. The present specimen has a basal cavity greatly expanding beneath the lateral processes, thus resembling *A. transitans*; however, both the inner and outer terminations are not bluntly rounded but somewhat pointed, especially the outer one. Specimens with a similar shape of the lateral terminations of the basal cavity were also illustrated as *A. transitans* by Schönlaub (1980, pl. 4, fig. 17) and Valenzuela-Ríos (1994a, pl. 2, figs. 5, 8, 16).

Genus *Flajsella* Valenzuela-Ríos and Murphy, 1997

Type species.—*Spathognathodus stygius* Flajs, 1966.

Flajsella stygia (Flajs, 1966)
Figure 3.3–3.5

1966 *Spathognathodus stygius* Flajs, p. 204, pl. 5, figs. 16, 17.
1968 *Pathognathodus seebergensis* Schulze, p. 227, pl. 17, fig. 4.
1979 *Ozarkodina stygia* (Flajs); Lane and Ormiston, p. 57, pl. 1, figs. 45, 46, pl. 2, figs. 10, 11.
1983 *Ozarkodina stygia* (Flajs); Murphy and Matti, p. 10, pl. 3, figs. 1, 2, 7, 8.
1983 *Ozarkodina stygia* (Flajs); Wang and Ziegler, pl. 2, fig. 1.
1994a *Ozarkodina stygia* (Flajs); Valenzuela-Río, p. 66, pl. 6, figs. 17–19.

https://doi.org/10.1017/jpa.2021.108 Published online by Cambridge University Press

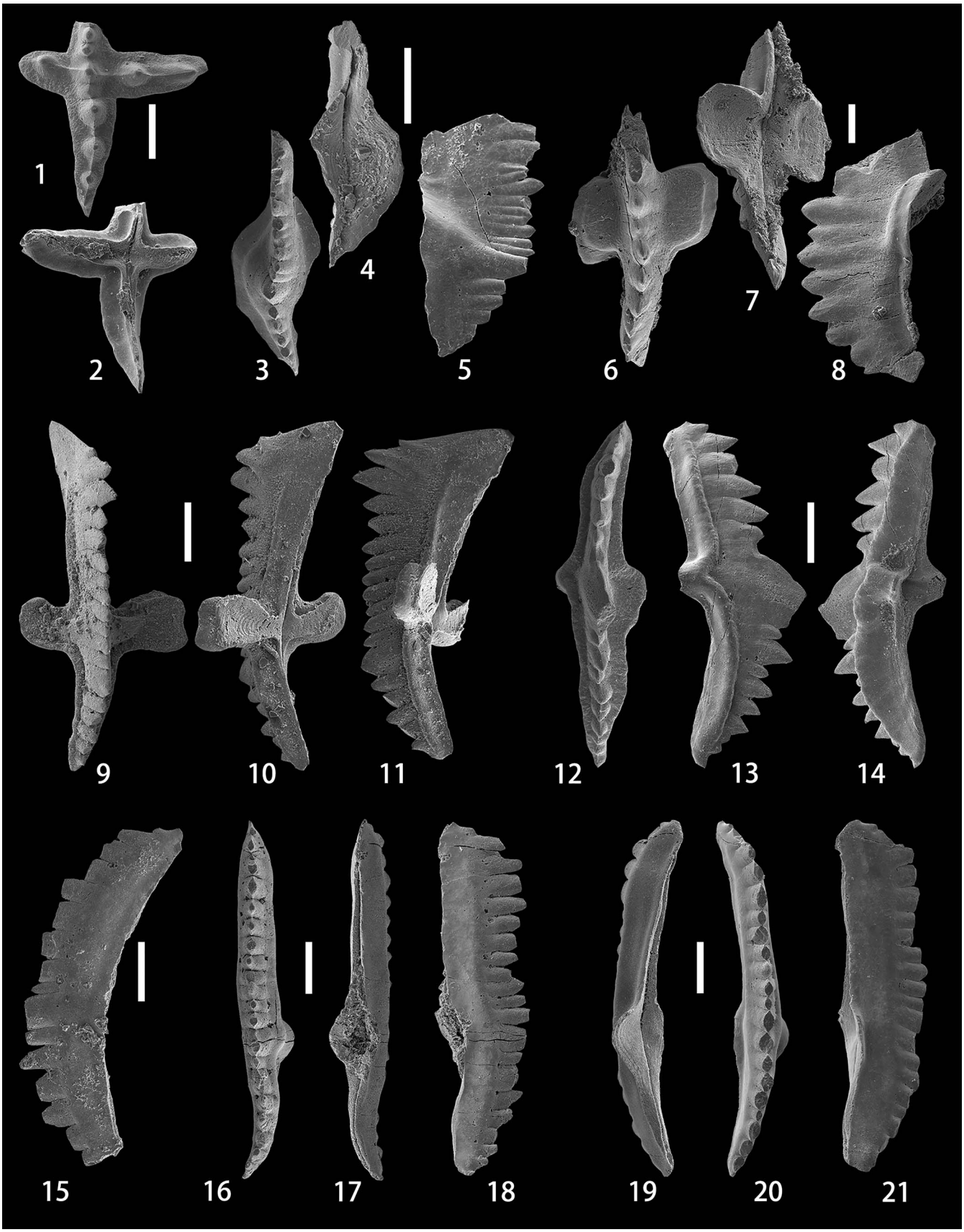

https://doi.org/10.1017/jpa.2021.108 Published online by Cambridge University Press

Figure 3. (**1, 2**) *Ancyrodelloides transitans* (Bischoff and Sannemann, 1958), upper and lower views of the Pa element, NIGP 175046, sample ALC-12-6m. (**3–5**) *Flajsella stygia* (Flajs, 1966), upper, lower, and lateral views of the Pa element, NIGP 175047, sample ALC-12-10m. (**6–8**) *Lanea omoalpha* Murphy and Valenzuela-Ríos, 1999, upper, lower, and lateral views of the Pa element, NIGP 175048, sample ALC-11-3m. (**9–14**) *Lanea telleri* (Schulze, 1968); (**9–11**) upper, lower, and lateral views of the Pa element, NIGP 175049, sample ALC-12-10m; (**12–14**) upper, lateral, and lower-lateral views of the Pb element, NIGP 175050, sample ALC-12-10m. (**15**) *Wurmiella excavata* (Branson and Mehl, 1933), lateral view of the Pa element, NIGP 175051, sample ALC-10-19m. (**16–18**) *Wurmiella tuma* (Murphy and Matti, 1983), upper, lower, and lateral views of the Pa element, NIGP 175052, sample ALC-11-9m. (**19–21**) *Wurmiella* aff. *W. tuma* (Murphy and Matti, 1983), lower, upper, and lateral views of the Pa element, NIGP 175053, sample ALC-12-6m. All scale bars represent 200 µm.

1997 *Flajsella stygia* (Flajs); Valenzuela-Ríos and Murphy, p. 139, figs. 8.26–8.28, ?9.17, 9.18, 9.26–9.30. [with synonymy list]
1998 *Flajsella stygia* (Flajs); Valenzuela-Ríos and García-López, pl. 1, fig. 4.
2002 *Flajsella stygia* (Flajs); Valenzuela-Ríos, pl. 1, fig. 8.
2007 *Flajsella stygia* (Flajs); Suttner, p. 31, pl. 18, figs. 12, 13.
2017 *Flajsella stygia* (Flajs); Murphy and Valenzuela-Ríos, pl. 1, figs. 1–5, 25, 28, 29.
2017 *Flajsella stygia* (Flajs); Schönlaub et al., pl. 3, figs. 5, 6.
2017 *Flajsella stygia* (Flajs); Takahashi et al., p. 994, fig. 5.9.
2017a *Flajsella stygia* (Flajs); Valenzuela-Ríos et al., fig. 6.5.
2019 *Flajsella stygia* (Flajs); Corradini et al., fig. 12G.

Holotype.—Specimen 2337/115/1 from the limestone at 1280 m from the south portal of the Plöcken tunnel, Carnic Alps, Austria (Flajs, 1966, pl. 5, fig. 17).

Description.—The anterior part of the free blade is broken; the straight posterior part clearly bends to join the cusp at the proximal end. The posterior carina joins the anterior carina at the cusp in an obvious offset. In front of the stout cusp, characterized by an elliptical cross-section, the remnant of the anterior blade consists of two comparatively wider and probably higher denticles anteriorly and nine narrower and smaller denticles posteriorly that are of approximately the same height. Therefore, the highest point of the blade probably lies in the anterior half of the anterior carina. The short posterior carina is slightly deflected inwards, and is composed of four denticles descending steeply from the cusp. The basal cavity is large and deep, with a broken inner lobe. The lower margin in the posterior part of the blade is characteristically straight.

Material.—One specimen from sample ALC-12-10m.

Remarks.—Although the anterior part of the anterior blade is broken, the obvious offset of the straight anterior carina and slightly deflected posterior carina at the cusp, the steeply descending posterior denticles, and the highest point of the blade probably located in the anterior half of the anterior blade permit assignment of our specimen to *F. stygia*. *Flajsella schulzei* (Bardashev, 1989) differs from *F. stygia* in the straight anterior carina that is in line with the posterior carina, and the almost symmetrical basal cavity. *Flajsella stygia* also shares a close similarity in the outline of the carinae around the cusp with *F. streptostygia* Valenzuela-Ríos and Murphy, 1997, which, however, is highly distinguishable by the curved anterior carina and the angular junction of carinae at the cusp.

Genus *Lanea* Murphy and Valenzuela-Ríos, 1999

Type species.—*Ozarkodina eleanorae* Lane and Ormiston, 1979.

Lanea omoalpha Murphy and Valenzuela-Ríos, 1999
Figure 3.6–3.8

1983 *Ancyrodelloides omus* alpha morph Murphy and Matti, p. 16, pl. 2, figs. 18–20.
?1994 *Ancyrodelloides omus* alpha morph Murphy and Matti; Mawson and Talent, p. 51, figs. 11H–L.
1994a *Ancyrodelloides omus* morphotype delta Valenzuela-Ríos, p. 40, pl. 1, fig. 10.
1999 *Lanea omoalpha* Murphy and Valenzuela-Ríos, p. 327, pl. 1, figs. 10–19, 23, 27–29, pl. 2, figs. 12–14.
1999 *Ancyrodelloides omus* Murphy and Matti; Talent and Mawson, p. 73, pl. 5, figs. 6, 7, 9, pl. 7, fig. 13, pl. 12, fig. 10.
2000 *Ancyrodelloides omus* Murphy and Matti; Wang et al., pl. 2, fig. 5.
2002 *Lanea omoalpha* Murphy and Valenzuela-Ríos; García-López et al., pl. 3, fig. 11.
2004 *Lanea omoalpha* Murphy and Valenzuela-Ríos; Farrell, p. 976, pl. 8, figs. 12, 13.
2005 *Lanea omoalpha* Murphy and Valenzuela-Ríos; Barrick et al., p. 117, pl. 1, figs. 5–8, 13, 14.
non 2005 *Lanea omoalpha* Murphy and Valenzuela-Ríos; Jin et al., pl. 2, figs. 6–8, 11, 12.
2005 *Lanea omoalpha* Murphy and Valenzuela-Ríos; Valenzuela-Ríos et al., pl. 1, figs. e, f.
2005b *Lanea omoalpha* Murphy and Valenzuela-Ríos; Wang et al., fig. 3.3, 3.4.
2006 *Lanea omoalpha* Murphy and Valenzuela-Ríos; Wang, p. 214, pl. 4, figs. 1, 2, pl. 5, figs. 4, 5, 8, 9.
non 2007 *Lanea omoalpha* Murphy and Valenzuela-Ríos; Jansen et al., fig. 3.6.
2007 *Lanea omoalpha* Murphy and Valenzuela-Ríos; Suttner, p. 31, pl. 19, figs. 5, 8. 10.
2009 *Lanea omoalpha* Murphy and Valenzuela-Ríos; Wang et al., pl. 2, fig. 22.
2012 *Lanea omoalpha* Murphy and Valenzuela-Ríos; Drygant and Szaniawski, p. 858, fig. 13M, P, T.
2012 *Lanea* cf. *omoalpha* Murphy and Valenzuela-Ríos; Slavík et al., fig. 6.14.
2013 *Lanea omoalpha* Murphy and Valenzuela-Ríos; Mavrinskaya and Slavík, fig. 5A–C.
?2016 *Lanea omoalpha* Murphy and Valenzuela-Ríos; Corriga et al., fig. 5Q.
2016 *Ancyrodelloides omus* Murphy and Matti; Mathieson et al., p. 614, fig. 21A–F.

https://doi.org/10.1017/jpa.2021.108 Published online by Cambridge University Press

2017 *Lanea omoalpha* Murphy and Valenzuela-Ríos; Schönlaub et al., pl. 3, fig. 20.
2017 *Lanea omoalpha* Murphy and Valenzuela-Ríos; Valenzuela-Ríos and Liao, fig. 4.2, 4.3.
2017b *Lanea omoalpha* Murphy and Valenzuela-Ríos; Valenzuela-Ríos et al., fig. 4.8.
2019 *Lanea omoalpha* Murphy and Valenzuela-Ríos; Corradini et al., fig.12Q.
2020 *Lanea omoalpha* Murphy and Valenzuela-Ríos; Hušková and Slavík, fig. 7D.
2020 *Lanea omoalpha* Murphy and Valenzuela-Ríos; Medici et al., fig. 2H.

Holotype.—Specimen UCR 8762, I/1, from the Windmill Limestone at SP VII Section, Coal Canyon, northern Simpson Park Range, Nevada, USA (Murphy and Valenzuela-Ríos, 1999, pl. 1, figs. 17–19).

Description.—The anterior blade is broken, only the last denticle, characterized by a lenticular cross-section, was preserved. The posterior blade consists of seven denticles that descend gradually from the second denticle to the posterior end, thus forming an arched upper profile in lateral view. Situated above the apex of the basal cavity, the cusp is slightly enlarged but not prominently high. Platform lobes are slightly asymmetrical and characteristically subquadrate-rounded, with a well-developed terrace extending from the blade at ~90° on both sides and meeting the brim, which is much smaller and narrower than the terrace, at an obtuse angle. The wide and open basal cavity extends anteriorly beneath the anterior blade as an open and deep groove, and posteriorly as an open but somewhat shallow groove that gradually tapers to the posterior termination. In lateral view, a weak pinch zone is developed close to the lower margin of the anterior and posterior blades.

Material.—One specimen from sample ALC-11-3m.

Remarks.—The broken specimen depicted herein is quite large (1.33 mm long) and probably represents an ontogenetically gerontic form. The arrangement of enlarged denticles on the posterior blade, the unconstricted large basal cavity, the large platform terrace that joins the brim at an obtuse angle, and the weakly developed pinch zone allow the identification of this broken specimen as *L. omoalpha*. The specimen closely resembles one broken specimen illustrated by Murphy and Valenzuela-Ríos (1999, pl. 2, figs. 12–14) in the arrangement of denticles on the blade and the lower and upper profiles of the blade. This specimen resembles *L. eoeleanorae* Murphy and Valenzuela-Ríos, 1999, in possessing a well-developed terrace that occupies most of the lobe surface; however, the obtuse angle junction of the terrace and brim, the clearly visible platform lobes in oral view, and the absence of a distinct brim sulcus in lateral view differ from the corresponding features of *L. eoeleanorae*.

Lanea telleri (Schulze, 1968)
Figure 3.9–3.14

1968 *Spathognathodus steinhornensis telleri* Schulze, p. 229, pl. 17, figs. 18, 19.
1999 *Lanea telleri* (Schulze); Murphy and Valenzuela-Ríos, p. 330, pl. 2, figs. 24–40. [with synonymy list]
2002 *Lanea telleri* (Schulze); Valenzuela-Ríos, pl. 1, fig. 6.
2007 *Lanea telleri* (Schulze); Suttner, p. 32, pl. 19, figs. 11, 12.
2016 *Lanea telleri* (Schulze); Corradini et al., pl. 3, fig. 10.
2017 *Lanea telleri* (Schulze); Schönlaub et al., pl. 3, fig. 18.
2017a *Lanea telleri* (Schulze); Valenzuela-Ríos et al., fig. 6.3.

Holotype.—Specimen Tüb. Co 1313/37 from P. 10/Probe 1 at Seeberggebiet, Karawanken Alps, southern Austria (Schulze, 1968, pl. 17, fig. 19).

Description.—The robust Pa element is deflected slightly inwards in the posterior part and arched gently downwards anteriorly and posteriorly, thus the anterior and posterior ends of the lower margin are the lowest. At the anterior end of the blade, there are two high denticles, which are followed by about nine palisade-type and almost uniform (in height rather than in width) denticles anteriorly, and six gradually descending denticles posteriorly. The cusp is not prominent, but the first denticle on the posterior blade is enlarged. Located entirely posterior to the middle point of the blade, the terraced platform lobes are asymmetrical, thus the rectangular outer lobe is much wider than the semi-circular inner lobe. The anterior blade is longer than the posterior blade. The edge of the platform is rimmed by a narrow marginal ridge, which extends along margins of the anterior and posterior ledges. On the lower side, the constricted basal cavity is dumbbell shaped, extending anteriorly and posteriorly as appressed grooves.

The angulate pectiniform Pb element is as robust as the Pa element, and slightly deflected laterally at the anterior end. The posteriorly reclined cusp is extremely wide and high, anterior to which are six palisade, back-curved, and more or less uniform denticles, and posterior to which are eight irregular and comparatively smaller denticles. The anterior process is as long as the posterior one. A narrow and asymmetrical platform is developed on the inner and outer sides of the blade, and extends along the anterior and posterior processes as a bench at the base of the denticles. On the lower side, the basal cavity is also constricted and runs anteriorly and posteriorly as appressed grooves.

Material.—One Pa element and one Pb element from sample ALC-12-10m.

Remarks.—Our Pa element conforms to the description of the Pa element given by Murphy and Valenzuela-Ríos (1999, p. 332) in having a constricted basal cavity, a rimed platform, well-developed benches along the anterior and posterior blades, and a posteriorly situated basal cavity. Murphy and Valenzuela-Ríos (1999) also illustrated two specimens of Pb element from the Simpson Park Range section VII, which our Pb element closely resembles in possessing benches on the anterior and posterior processes. However, our specimen differs in having fewer but stouter denticles anterior to the wide and high cusp.

Genus *Wurmiella* Murphy, Valenzuela-Ríos, and Carls, 2004

https://doi.org/10.1017/jpa.2021.108 Published online by Cambridge University Press

Type species.—*Ozarkodina excavata tuma* Murphy and Matti, 1983.

Wurmiella excavata (Branson and Mehl, 1933)
Figure 3.15

1933 *Ozarkodina simplex* Branson and Mehl, p. 52, pl. 3, figs. 46, 47.
1983 *Ozarkodina excavata excavata* (Branson and Mehl); Wang, p. 154, pl. 1, figs. 10, 11, 14–16, pl. 2, figs. 24, 25.
2005a *Ozarkodina excavata excavata* (Branson and Mehl); Wang et al., pl. 1, fig. 2.
2009 *Wurmiella excavatus* (Branson and Mehl); Corriga and Corradini, fig. 4C.
2009 *Ozarkodina excavata excavata* (Branson and Mehl); Suttner, p. 78, pl. 1, fig. 15. [with synonymy list]
2010 *Wurmiella excavata* (Branson and Mehl); Corradini and Corriga, p. 248, pl. 2, figs. 9–25.
2014b *Wurmiella excavata* (Branson and Mehl); Corriga et al., fig. 6A.
2016 *Wurmiella excavata* (Branson and Mehl); Corradini et al., pl. 3, figs. 14, 15, pl. 4, figs. 1, 2.
2017 *Wurmiella excavata* (Branson and Mehl); Schönlaub et al., pl. 2, fig. 3.
2017 *Wurmiella excavata* (Branson and Mehl); Takahashi et al., p. 995, fig. 5.12, 5.13.
2020 *Wurmiella excavata* (Branson and Mehl); Chen et al., figs. 5bb, cc, 6a–c, e, f, 7o–q, t.
2020 *Wurmiella excavata* (Branson and Mehl); Hušková and Slavík, fig. 7H.

Neotype.—Specimen 13151 from the Bainbridge Formation at Lithium, Missouri, USA (Rexroad and Crag, 1971, pl. 80, fig. 7).

Description.—Specimens of the Pa element have a long, straight or twisted blade bearing 11–15 denticles (partially broken posteriorly in some specimens), and are usually arched downwards posteriorly, resulting in a rounded lower margin in lateral view. The irregular denticles are normally stout or palisade, and erect or posteriorly reclined. The cusp is slightly or remarkably wider than other denticles and situated in the posterior half. The small lobes are slightly to clearly asymmetrical (in some specimens one lobe is more developed and laterally extended than the opposite lobe). The small and moderately deep basal cavity extends anteriorly as an open and slightly deep groove that turns to be appressed at the anterior termination of the blade, and posteriorly as an open but somewhat shallow groove that may be inverted at the posterior end. In lateral view, ledges are absent or weakly developed at the base of the denticles.

Material.—Eight specimens from samples ALC-9-4m (1), ALC-10-19m (3), and ALC-10-23m (4).

Remarks.—This species shares a close similarity with *W. tuma* (Murphy and Matti, 1983) and *W. wurmi* (Bischoff and Sannemann, 1958). However, *W. tuma* differs from *W. excavata* in having a higher density of denticles on the blade, poorly developed cusp, and strongly developed ledges at the base of denticles. *Wurmiella wurmi* differs from *W. excavata* in possessing a biconcave or convexo-concave lower margin and well-developed ledges.

Wurmiella tuma (Murphy and Matti, 1983)
Figure 3.16–3.18

1982 *Spahognathodus wurmi* Bischoff and Sannemann; Wang, p. 445, pl. 1, figs. 25–27, 29, 30.
1983 *Ozarkodina excavata tuma* Murphy and Matti, p. 7, pl. 1, figs. 3–9.
1986 *Ozarkodina tuma* Murphy and Matti; Murphy and Cebecioglu, pl. 1, fig. 1.1–1.7, 1.18–1.22.
1994a *Ozarkodina tuma* Murphy and Matti; Valenzuela-Ríos, p. 70, pl. 4, figs. 2, 5.
2004 *Wurmiella tuma* (Murphy and Matti); Murphy et al., p. 11, fig. 2.16–2.28.

Holotype.—Specimen UCR8536/2 from the Bastille Limestone at the Mill Canyon Section, central Nevada, USA (Murphy and Matti, 1983, pl. 1, figs. 3, 4).

Description.—Specimens of the Pa element are long and consist of 20 small and palisade denticles of a lenticular cross-section, of which the straight anterior blade and weakly or clearly deflected posterior blade bear 12 and 8 denticles, respectively. Two to three denticles close to the anterior end of the blade and the cusp posterior to the middle point of the blade are somewhat enlarged, but not prominently high. The lower margin is characteristically stepped. The slightly deep and asymmetrical basal cavity, with small, inflated, and shouldered lobes, is situated posterior to the mid-length of the blade. The basal cavity extends anteriorly as an open and deep groove, reaching the anterior end of the blade, and posteriorly for a short distance as a flush groove, which is followed by a clearly inverted keel to the posterior end. In lateral view, ledges are strongly developed on both sides of the blade at the base of denticles.

Material.—Four specimens from samples ALC-11-9m (1), ALC-12-6m (1), and ALC-13-13m (2).

Remarks.—Specimens are similar to the representative Pa elements of *W. tuma* in the high number of denticles on the blade, the well-developed ledges, the asymmetrical and deep basal cavity with inflated lobes, and the straight or angular lower margin. According to Murphy and Matti (1983, pl. 1, figs. 3–9), representative Pa elements of *W. tuma* have an open and deep posterior groove tapering to the end; in contrast, the illustrated specimen herein differs slightly in the development of a short groove that turns into an inverted keel at the end of the posterior blade. On the basis of the profile of the lower margin, *W. tuma* differs greatly from *W. wurmi*.

The ledges and inner shoulder in one specimen provisionally designated here as *W.* aff. *W. tuma* (Fig. 3.19–3.21) are weakly or barely developed, as opposed to *W. tuma* in which the ledges and inner shoulder are strongly developed. Moreover, the basal cavity of *W.* aff. *W. tuma* is shallow and extends posteriorly as a clearly inverted keel. Both of these features differ greatly from the corresponding features of *W. tuma*.

https://doi.org/10.1017/jpa.2021.108 Published online by Cambridge University Press

Genus *Zieglerodina* Murphy, Valenzuela-Ríos, and Carls, 2004

Type species.—*Spathognathodus remscheidensis* Ziegler, 1960.

Zieglerodina eladioi (Valenzuela-Ríos, 1994a)
Figure 4.1–4.8

1983 *Ozarkodina remscheidensis remscheidensis* (Ziegler); Wang, p. 155, pl. 2, fig. 22.
1994a *Ozarkodina eladioi* Valenzuela-Ríos, p. 59, pl. 5, figs. 1–35. [with synonymy list]
2006 "*Ozarkodina*" *eladioi* Valenzuela-Ríos; Sanz-López et al., fig. 5.14, 5.15.
2007 *Ozarkodina remscheidensis remscheidensis* (Ziegler); Benfrika et al., fig. 8A.
2016 *Zieglerodina eladioi* (Valenzuela-Ríos); Corriga et al., p. 266, fig. 5A, B.
2017 *Zieglerodina eladioi* (Valenzuela-Ríos); Schönlaub et al., pl. 3, fig. 2.
2019a *Zieglerodina eladioi* (Valenzuela-Ríos); Corriga and Corradini, p. 182, figs. 2, 3.
2020 *Zieglerodina eladioi* (Valenzuela-Ríos); Corradini et al., fig. 12C.

Holotype.—Specimen MPZ 8072 from Bed 6A of Litosoma A at the Gerri 1.1 Section, Spanish Central Pyrenees (Valenzuela-Ríos, 1994a, pl. 5, fig. 1).

Description.—Specimens of the Pa element have a short posterior blade bearing four denticles, the anteriormost one of which is usually small and followed by two higher and larger denticles before a lowest and small denticle at the posterior end. The anterior blade constitutes 5–6 denticles that are of similar size and of more or less the same height, except for the anteriormost one or two, which may be slightly higher. The high cusp is almost twice as wide as adjacent denticles, but only slightly wider than the stoutest denticle on the posterior blade. Normally, the axis of the blade is straight. The basal cavity, which is situated posterior to the middle length of the blade, has two wide, asymmetrical, and strongly expanded lateral lobes. The basal cavity extends anteriorly as a narrow and deep groove reaching the anterior end of the blade, and as a wide and deep groove tapering towards the posterior end.

Material.—Seven specimens from samples ALC-10-15m (1), ALC-10-19m (2), and ALC-10-23m (4).

Remarks.—According to the original description introduced by Valenzuela-Ríos (1994a), *Z. eladioi* is mainly characterized by the short posterior blade possessing two larger denticles, a comparably longer anterior blade whose denticles vary little in size, and two wide, slightly asymmetrical lobes, all of which are clearly observed in our specimens. A great many specimens of this species were previously identified as *Z. remscheidensis* (Ziegler, 1960), which, however, has distinctly high and strong denticles at the anterior end of the blade and more numerous denticles on the blade. *Zieglerodina mashkovae* (Drygant, 1984) differs greatly from *Z. eladioi* in possessing straight upper and lower margins, a symmetrical and approximately centrally situated basal cavity, numerous (5–7) denticles of nearly equal height on the anterior and posterior blades, and a large cusp. *Zieglerodina shoenlaubi* Corradini et al., 2019, which resembles *Z. eladioi* in possessing a short posterior blade, is distinguishable by having small denticles alternating with large ones on the blade.

Zieglerodina planilingua (Murphy and Valenzuela-Ríos, 1999)
Figure 4.9–4.14

1982 *Spathognathodus remscheidensis* Ziegler; Wang, p. 444, pl. 1, figs. 13, 14.
1999 "*Ozarkodina*" *planilingua* Murphy and Valenzuela-Ríos, p. 326, pl. 1, figs. 1–9.
2002 *Ozarkodina planilingua* Murphy and Valenzuela-Ríos; García-López et al., pl. 3, fig. 10.
2003 "*Ozarkodina*" *planilingua* Murphy and Valenzuela-Ríos; Farrell, p. 137, pl. 7, figs. 20–23.
2005 *Ozarkodina planilingua* Murphy and Valenzuela-Ríos; Barrick et al., p. 120, pl. 1, figs. 3, 4, 11, 12.
? 2005a "*Ozarkodina*" *planilingua* Murphy and Valenzuela-Ríos; Wang et al., pl. 1, figs. 10, 15.
2005b "*Ozarkodina*" *planilingua* Murphy and Valenzuela-Ríos; Wang et al., fig. 3.5, 3.6.
2006 *Lanea omoalpha* Murphy and Valenzuela-Ríos; Wang, p. 214, pl. 5, figs. 12–15.
2009 *Ozarkodina planilingua* Murphy and Valenzuela-Ríos; Corriga and Corradini, fig. 4J, K.
2010 *Ozarkodina planilingua* Murphy and Valenzuela-Ríos; Corradini and Corriga, pl. 3, figs. 14–16.
2012 *Zieglerodina planilingua* (Murphy and Valenzuela-Ríos); Drygant and Szaniawski, p. 856, fig. 13A–D.
2014a *Zieglerodina planilingua* (Murphy and Valenzuela-Ríos); Corriga et al., fig. 3C.
2014b *Zieglerodina planilingua* (Murphy and Valenzuela-Ríos); Corriga et al., p. 197, fig. 6H–L.
2016 *Zieglerodina planilingua* (Murphy and Valenzuela-Ríos); Corradini et al., pl. 3, fig. 12.
2016 *Zieglerodina planilingua* (Murphy and Valenzuela-Ríos); Corriga et al., fig. 5O.
2017 "*Ozarkodina*" *planilingua* Murphy and Valenzuela-Ríos; Zhen et al., fig. 5a, ?b.
2018 *Lanea planilingua* (Murphy and Valenzuela-Ríos); Wang et al., fig. 4A–F.
2020 *Lanea planilingua* (Murphy and Valenzuela-Ríos); Hušková and Slavík, fig. 7E.
2020 *Zieglerodina planilingua* (Murphy and Valenzuela-Ríos); Medici et al., fig. 2L.
2020 *Zieglerodina planilingua* (Murphy and Valenzuela-Ríos); Corradini et al., fig. 12J.

Holotype.—Specimen UCR 8758, I/3, from the Windmill Limestone at SP VII Section, Coal Canyon, northern Simpson Park Range, Nevada, USA (Murphy and Valenzuela-Ríos, 1999, pl. 1, figs. 7–9).

https://doi.org/10.1017/jpa.2021.108 Published online by Cambridge University Press

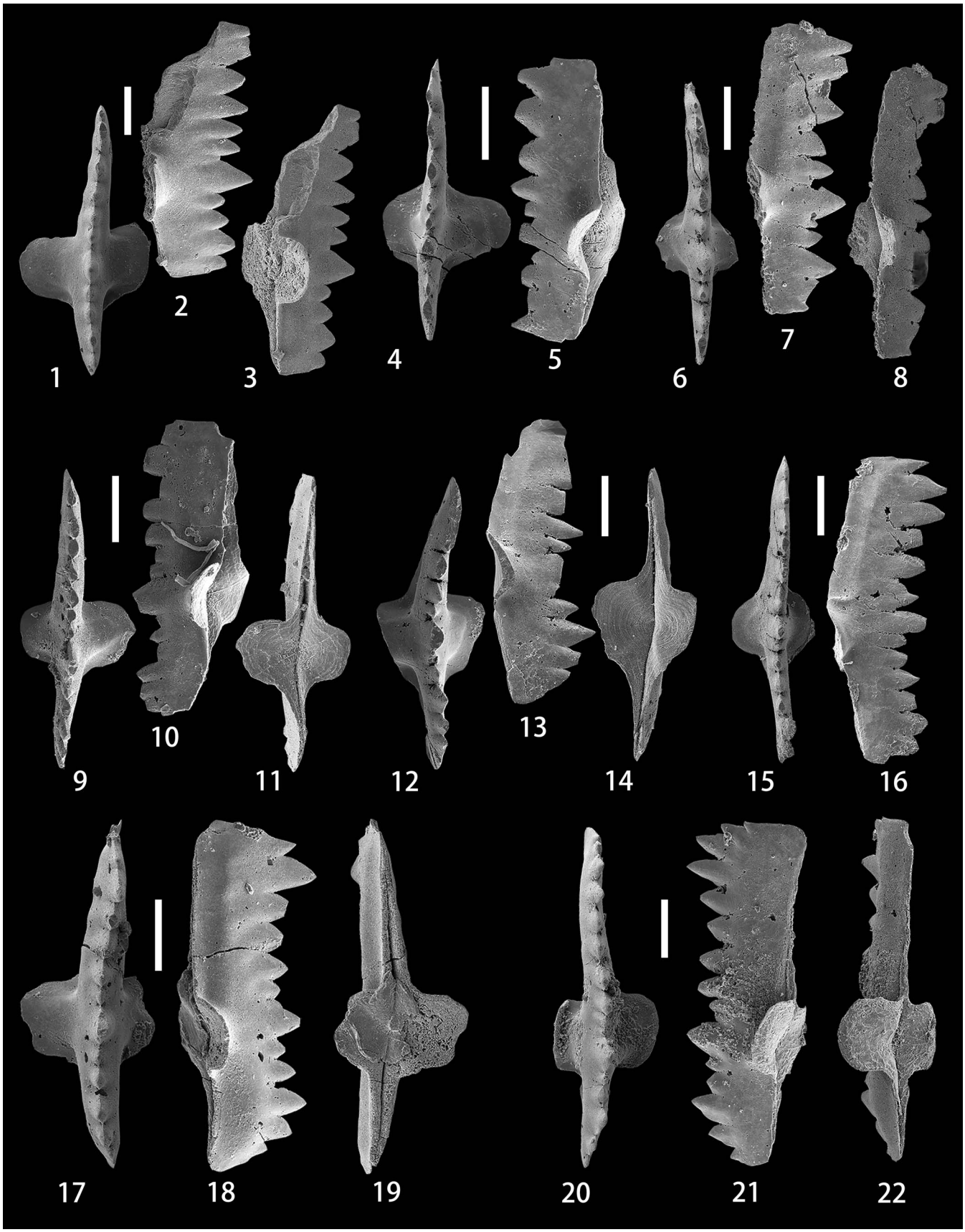

https://doi.org/10.1017/jpa.2021.108 Published online by Cambridge University Press

Figure 4. (**1–8**) *Zieglerodina eladioi* (Valenzuela-Ríos, 1994a); (**1–3**) upper, lateral, and lower-lateral views of the Pa element, NIGP 175054, sample ALC-10-19m; (**4, 5**) upper and lower-lateral views of the Pa element, NIGP 175055, sample ALC-10-23m; (**6–8**) upper, lateral, and lower-lateral views of the Pa element, NIGP 175056, sample ALC-10-23m. (**9–14**) *Zieglerodina planilingua* (Murphy and Valenzuela-Ríos, 1999); (**9–11**) upper, lateral, and lower views of the Pa element, NIGP 175057, sample ALC-9-10m; (**12–14**) upper, lateral, and lower views of the Pa element, NIGP 175058, sample ALC-10-23m. (**15–22**) *Zieglerodina remscheidensis* (Ziegler, 1960); (**15, 16**) upper and lateral views of the Pa element, NIGP 175059, sample ALC-10-2m; (**17–19**) upper, lateral, and lower views of the Pa element, NIGP 175060, sample ALC-10-19m, the width and height of the cusp are reduced because of breakage; (**20–22**) upper, lateral, and lower views of the Pa element, NIGP 175061, sample ALC-10-23m. All scale bars represent 200 µm.

Description.—Specimens of the Pa element are usually straight and consist of 11–16 stout denticles of a lenticular cross-section. At the anterior end of the blade, there are 2–3 high denticles followed by 3–5 smaller and lower denticles before the prominent and enlarged cusp. Posterior to the cusp are one or two small denticles, which are succeed posteriorly by three larger and higher denticles. The denticle at the posterior end of the blade is the lowest. The slightly asymmetrical, semi-circular or subquadrate-rounded lobes have a small terrace that extends from the blade at various angles and meet the brim at an obtuse angle, and are positioned slightly posterior to the middle length of the blade. In all specimens, the brim surface of the lobe is larger than the terrace. The basal cavity is wide, moderately deep, and unconstricted, extending anteriorly and posteriorly as deep grooves that taper gradually to distal ends. In lateral view, a weak pinch zone is present close to the lower margin of the blade.

Material.—Seven specimens from samples ALC-9-10m (1), ALC-10-6m (1), and ALC-10-23m (5).

Remarks.—The arrangement of the denticles on the blade, the outline of the basal cavity, and the development and shape of the terrace allow us to assign our specimens to *Z. planilingua*. This species is morphologically like *Z. remscheidensis* and *L. omoalpha*, the former of which does not possess the wide basal cavity and the characteristic small terrace on lobes, whereas the latter of which has a more developed and larger terrace than *Z. planilingua*. Moreover, the arrangement of denticles on the posterior blade in *L. omoalpha* is different from that in *Z. planilingua*.

Zieglerodina remscheidensis (Ziegler, 1960)
Figure 4.15–4.22

1960 *Spathognathodusremscheidensis* Ziegler, p. 194, pl. 13, figs. 1, 2, 4, 5, 7, 8, 10, 14.
1964 *Spathognathodus steinhornensis remscheidensis* Ziegler; Walliser, p. 87, pl. 9, fig. 24.
non 1966 *Spathognathodusremscheidensis* Ziegler; Clark and Ethington, pl. 84, figs. 12, 14.
non 1969 *Spathognathodus steinhornensisremscheidensis* Ziegler; Fåhræus, pl. 1, figs. 12, 15, 16.
non 1970 *Spathognathodusremscheidensis* Ziegler; Druce, p. 57, pl. 8, fig. ?4, pl. 9, fig. 9.
non 1971 *Spathognathodusremscheidensis* Ziegler; Barnett, p. 288, pl. 35, figs. 1–20, pl. 36, figs. 1–24.
1972 *Spathognathodus steinhornensis* Ziegler; Link and Druce, p. 92, pl. 10, figs. 1–7, text-fig. 60.
1972 *Spathognathodus steinhornensisremscheidensis* Ziegler; Mashkova, p. 83, pl. 2, fig. 20.
non 1973 *Spathognathodusremscheidensis* Ziegler; Savage, p. 329, pl. 34, figs. 9–29, 33–42, text-fig. 28.
1975 *Ozarkodina remscheidensis remscheidensis* (Ziegler); Klapper and Murphy, p. 41, pl. 7, figs. 22, 25–30.
non 1975 *Ozarkodina remscheidensis* (Ziegler); Carls, pl. 2, figs. 16–18.
non 1976 *Ozarkodina remscheidensis remscheidensis* (Ziegler); Mehrtens and Barnett, p. 497, pl. 1, figs. 7, 10.
1977 *Ozarkodina remscheidensis remscheidensis* (Ziegler); Chatterton and Perry, p. 786, pl. 3, figs. 28–32; pl. 4, fig. 36.
non 1979 *Spathognathodus* cf.remscheidensis Ziegler; Wang, p. 403, pl. 1, figs. 23, 24.
1980 *Ozarkodina remscheidensis remscheidensis* (Ziegler); Chlupáč et al., pl. 18, figs. 11, 14–26, pl. 19, figs. 7, 13, 14, 18–21.
non 1980 *Ozarkodina remscheidensis* (Ziegler); Pickett, fig. 13D–G.
1980 *Ozarkodina remscheidensis remscheidensis* (Ziegler); Schönlaub, pl. 1, figs. 8, ?15, pl. 3, fig. 21, pl. 4, fig. 2, pl. 6, fig. 4, pl. 7, fig. 29.
1980 *Ozarkodina remscheidensis remscheidensis* (Ziegler); Serpagli and Mastandrea, figs. 8, 12.
1980 *Ozarkodina remscheidensis remscheidensis* (Ziegler); Uyeno, p. 41, pl. 3, figs. 6, 7.
non 1981 *Spathognathodus remscheidensis* Ziegler; Wang, p. 81, pl. 1, figs. 1–6.
non 1982 *Ozarkodina remscheidensis* (Ziegler); Savage, p. 986, pl. 1, figs. 1–8, pl. 2, figs. 21–26.
1982 *Spathognathodus remscheidensis* Ziegler; Wang, p. 444, pl. 1, fig. 19.
1983 *Ozarkodina remscheidensis remscheidensis* (Ziegler); Wang, p. 155, pl. 2, fig. 26.
1983 *Ozarkodina remscheidensis* (Ziegler); Murphy and Matti, pl. 2, figs. 4–6.
1983 *Ozarkodina remscheidensis* (Ziegler); Wang and Ziegler, fig. 2.21.
1985a *Ozarkodina remscheidensis remscheidensis* (Ziegler); Mastandrea, p. 252, pl. 1, figs. 1–3.
1985b *Ozarkodina remscheidensis remscheidensis* (Ziegler); Mastandrea, pl. 1, fig. 1.
1985 *Ozarkodina remscheidensis remscheidensis* (Ziegler); Schönlaub, pl. 1, figs. 8, 9, 15.
1986 *Ozarkodina remscheidensis remscheidensis* (Ziegler); Mawson, p. 49, pl. 6, fig. 3.
1987 *Ozarkodina remscheidensis* (Ziegler); Kuwano, pl. 2, figs. 2, 3.
non 1987 *Ozarkodina remscheidensis remscheidensis* (Ziegler); Li, p. 364, pl. 164, figs. 1–4.
non 1989 *Ozarkodina steinhornensisremscheidensis* Ziegler; Jeppsson, p. 28, pl. 2, figs. 6–11.

https://doi.org/10.1017/jpa.2021.108 Published online by Cambridge University Press

non 1989 *Ozarkodina remscheidensis remscheidensis* (Ziegler); Sorentino, p. 93, pl. 3, figs. 1–9, 12, 13.
1989 *Ozarkodina remscheidensis remscheidensis* (Ziegler); Wilson, p. 139, pl. 11, figs. 8, 9.
non 1990 *Ozarkodina remscheidensis remscheidensis* (Ziegler); Bischoff and Argent, p. 457, pl. 4, figs. 1, ?2.
1990 *Ozarkodina remscheidensis remscheidensis* (Ziegler); Olivieri and Serpagli, pl. 4, fig. 10.
1990 *Ozarkodina remscheidensis* (Ziegler); Weyant and Morzadec, pl. 1, figs. 6, 7.
non 1990 *Ozarkodina remscheidensis remscheidensis* (Ziegler); Uyeno, p. 92, pl. 4, figs. 4–6, pl. 5, figs. 1–3, 30, 68, pl. 6, fig. 11, pl. 13, figs. 11, 12, 20, pl. 15, figs. 27, 28, 32–34, pl. 6, figs. 34, 35, pl. 17, figs. 10, 32.
non 1991 *Ozarkodina remscheidensis remscheidensis* (Ziegler); Uyeno, pl. 1, fig. 13.
non 1992 *Ozarkodina remscheidensis remscheidensis* (Ziegler); Barrick and Klapper, p. 49, pl. 4, figs. 8, 9, pl. 6, figs. 5–16.
non 1992 *Ozarkodina remscheidensis remscheidensis* (Ziegler); Bardashev and Ziegler, pl. 1, figs. 5, 6.
1994 *Ozarkodina remscheidensis remscheidensis* (Ziegler); Mawson and Talent, fig. 13O.
1994a *Ozarkodina remscheidensis remscheidensis* (Ziegler); Valenzuela-Ríos, p. 55. [with synonymy list]
1995 *Ozarkodina remscheidensis remscheidensis* (Ziegler); Barrick and Noble, fig. 6.9, 6.12, 6.15, 6.16.
non 1995 *Ozarkodina remscheidensis remscheidensis* (Ziegler); Colquhoun, pl. 1, figs. 9, 10.
non 1995 *Ozarkodina remscheidensis remscheidensis* (Ziegler); Sloan et al., pl. 12, figs. 9, 10.
1997 *Ozarkodina remscheidensis remscheidensis* (Ziegler); Miller and Aldridge, p. 46, pl. 1, figs. 21, 24.
non 1999 *Ozarkodina remscheidensis remscheidensis* (Ziegler); Talent and Mawson, pl. 5, figs. 13–18, pl. 7, fig. 12, pl. 8, fig. 1.
non 1999 *Ozarkodina remscheidensis remscheidensis* (Ziegler); Benfrika, p. 315, pl. 1, fig. 6.
2002 *Ozarkodina remscheidensis* (Ziegler); García-López et al., pl. 2, figs. 19, 20.
2003 *Ozarkodina remscheidensis remscheidensis* (Ziegler); Farrell, p. 137, pl. 8, figs. 1–4, 6, 8–15.
2003 *Ozarkodina remscheidensis remscheidensis* (Ziegler); Mawson et al., p. 90, pl. 2, figs. 2, 4–6, 10.
2004 *Ozarkodina remscheidensis remscheidensis* (Ziegler); Farrell, p. 974, pl. 10, figs. 2–4, 7–9.
2004 *Zieglerodina remscheidensis* (Ziegler); Murphy et al., p. 13, fig. 3.1–3.9, 3.11, ?3.14–3.16, 3.19, 3.20–3.25.
non 2005 *Ozarkodina remscheidensis* (Ziegler); Barrick et al., p. 120, pl. 1, figs. 2, 9, 10.
2005 *Ozarkodina remscheidensis remscheidensis* (Ziegler); Jin et al., pl. 2, figs. 9, 10.
non 2005 *Ozarkodina remscheidensis remscheidensis* (Ziegler); Trotter and Talent, p. 42, pl. 18, figs. 1, 3.
?2005 *Ozarkodina remscheidensis remscheidensis* (Ziegler); Corradini et al., fig. 5b.
2006 *Ozarkodina remscheidensis remscheidensis* (Ziegler); Wang, p. 212, pl. 5, figs. 10, 11.
non 2007 *Ozarkodina remscheidensis remscheidensis* (Ziegler); Benfrika et al., fig. 8A.
2007 *Ozarkodina remscheidensis remscheidensis* (Ziegler); Suttner, p. 41, pl. 17, figs. 7, 8, 10.
non 2008 *Ozarkodina remscheidensis remscheidensis* (Ziegler); Gaetani et al., p. 281, pl. 1, fig. 1.
2009 *Ozarkodina remscheidensis remscheidensis* (Ziegler); Suttner, p. 79, pl. 1, figs. 9, ?10.
2010 *Zieglerodina remscheidensis* (Ziegler); Corradini and Corriga, pl. 3, figs. 10, 11, ?12, 13.
2012 *Zieglerodina remscheidensis* (Ziegler); Corradini and Corriga, fig. 6H.
2012 *Zieglerodina remscheidensis* (Ziegler); Drygant and Szaniawski, p. 853, fig. 12A–G.
2014a *Zieglerodina remscheidensis* (Ziegler); Corriga et al., fig. 3G.
2014b *Zieglerodina remscheidensis* (Ziegler); Corriga et al., fig. 6F, G.
2016 *Zieglerodina remscheidensis* (Ziegler); Corradini et al., pl. 3, figs. 20–22.
2016 *Zieglerodina remscheidensis* (Ziegler); Corriga et al., fig. 5I, J.
2016 *Ozarkodina remscheidensis* (Ziegler); Mathieson et al., p. 634, figs. 27A–F, I, J, U, V, 32K.
non 2017 *Zieglerodina remscheidensis* (Ziegler); Zhen et al., fig. 5c, d.
2020 *Zieglerodina remscheidensis* (Ziegler); Corradini et al., fig. 12H.

Holotype.—Specimen G88b from the "Ockrige Kalke" of the basal part of the Hüinghäuser beds, Untenrüden Bed e, Rhenish Slate Mountains, Germany (Ziegler, 1960, pl. 13, fig. 4).

Description.—Specimens of the Pa element are normally straight or weakly deflected, and made up of 12–15 palisade or triangular denticles. At the anterior end of the blade is a small denticle, which is followed by one to two very high and wide denticles. The cusp is stout and prominent, but is not as high as the anteriormost denticles. Denticles between the high anteriormost part and the cusp are comparatively lower and smaller. The posterior blade possesses 5–6 denticles that vary in size, but all are lower than those at the anteriormost part of the blade. Two to three denticles posterior to the cusp are much smaller and lower, posterior to which is a high denticle, almost equal in height to the cusp. The basal cavity, occupying approximately one-quarter of the length of the blade, lies posterior to the middle point of the blade. Normally, it has rounded and symmetrical lobes that bear no ornamentation; however, an incipient and small terrace-like structure is present in some specimens (Fig. 4.15). Beneath the anterior and posterior blades, a narrow groove extends to distal ends of the blade. The lower margin is more or less straight, but the anterior lower margin may rise diagonally.

Material.—Eleven specimens from samples ALC-10-2m (2), ALC-10-15m (2), ALC-10-19m (2), and ALC-10-23m (5).

Remarks.—According to the original description given by Ziegler (1960), *Z. remscheidensis* is mainly characterized by

https://doi.org/10.1017/jpa.2021.108 Published online by Cambridge University Press

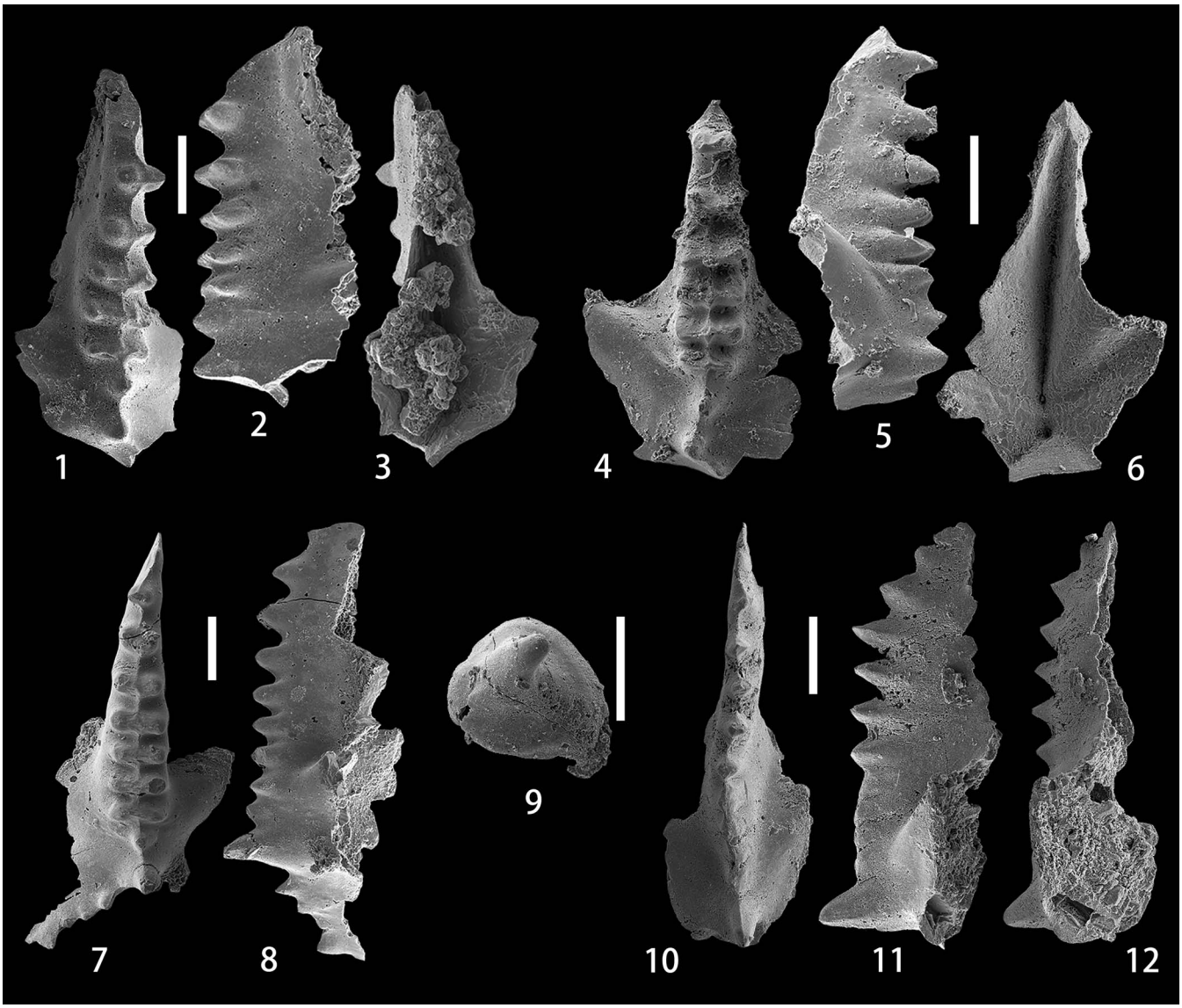

Figure 5. (**1–8**) *Caudicriodus* sp. B; (**1–3**) upper, lateral, and lower views of the I element, NIGP 175062, sample ALC-9-10m; (**4–6**) upper, lateral, and lower views of the I element, NIGP 175063, sample ALC-10-6m; (**7, 8**) upper and lateral views of the I element, NIGP 175064, sample ALC-10-19m. (**9**) *Pseudooneotodus beckmanni* (Bischoff and Sannemann, 1958), upper view, NIGP 175065, sample ALC-10-10m. (**10–12**) *Pelekysgnathus* sp. A, upper, lateral, and lower views of the I element, NIGP 175066, sample ALC-13-16m. All scale bars represent 200 µm.

having 1–2 denticles behind the anterior edge and a single denticle (the cusp) that is especially high above the basal cavity, and a basal cavity positioned in the anterior part of the posterior half of the blade.

Since first named by Ziegler (1960), *Z. remscheidensis* has been widely reported from the uppermost Silurian to the lowermost Devonian around the world. However, a great number of previously illustrated specimens do not conform to the representative specimens of this species, but have a centrally situated basal cavity and denticles on the blade of little variance in size and of the same height. In the establishment of the new genus *Zieglerodina*, Murphy et al. (2004) emphasized the common characteristics of this species and restricted its diagnosis to specimens morphologically resembling the holotype (Ziegler, 1960, pl. 13, fig. 4). In the present paper, the taxonomic revision proposed by Murphy et al. (2004) is adopted; therefore, the identification of specimens with more or less regular denticulation or a centrally positioned basal cavity as *Z. remscheidensis* is not accepted herein (for details, see the synonymy list).

Order Prioniodontida Dzik, 1976
Family Icriodontidae Müller and Müller, 1957
Genus *Caudicriodus* Bultynck, 1976

Type species.—*Icriodus woschmidti* Ziegler, 1960.

Caudicriodus sp. B
Figure 5.1–5.8

Description.—The I element has a narrow and long spindle that bears 4–7 transverse ridges posterior to the anteriormost denticle, is more or less straight, and gradually narrows

https://doi.org/10.1017/jpa.2021.108 Published online by Cambridge University Press

anteriorly in the anterior two-thirds, but keeps a constant width in the posterior one-third, thus resulting in a carrot-shaped outline. Median row denticles are distinct only in small specimens, but are completely fused with lateral row denticles in large ones. A weak or thin longitudinal crest runs from the anterior end of the spindle to the posterior end along the middle-line of the spindle. The transverse ridges in the posterior part of the spindle are separated by a constant and equal space, which becomes much greater in the anterior half of the spindle, especially between the first and second transverse ridges. Posterior to the spindle, two laterally compressed denticles are higher than those on the spindle. The first one is slightly or greatly smaller, from which an anteriorly directed and unornamented inner spur emanates. The posteriormost denticle is more prominent, from which a posteriorly directed process branches to the lateral side at an angle of ~120° with the main axis of the spindle. This outer process, which is moderately long (Fig. 5.7) or commonly broken (Fig. 5.1, 5.4), is denticulate and bears a well-developed thin ridge. On the lower side, the basal cavity is wide and deeply excavated in the posterior part.

Material.—Fifteen specimens from samples ALC-9-10m (5), ALC-10-2m (2), ALC-10-6m (4), ALC-10-10m (1), ALC-10-19m (1), and ALC-10-23m (2).

Remarks.—Our specimens are characterized by the numerous fused transverse ridges on the spindle, a feature normally observed in representative I elements of *C. hesperius* (Klapper and Murphy, 1975) and *C. woschmidti* (Ziegler, 1960). Unlike *C. woschmidti*, which has a short spindle with wide transverse ridges and a relatively restricted basal cavity, the Alengchu specimens possess a much narrower and longer spindle and a comparatively larger basal cavity. *Caudicriodus hesperius* is easily distinguishable by the extremely long posteriorly directed lateral process; in contrast, the posterior process is normally broken in most of the specimens (Fig. 5.1, 5.4) or much shorter in the intact specimen (Fig. 5.7). Moreover, the basal cavity in our specimens is less expanded than that of *C. hesperius*.

Genus *Pelekysgnathus* Thomas, 1949

Type species.—*Pelekysgnathus inclinatus* Thomas, 1949.

Pelekysgnathus sp. A
Figure 5.10–5.12

Description.—The specimen of the I element has a long and low blade bearing six small denticles in the anterior part, which is followed by an undenticulate and fused area that takes almost one-third of the length of the unit before a high, enlarged, and erect cusp at the posterior end. Three denticles at the anteriormost part are clearly proclined, whereas the following three denticles are more or less erect and of the same height. In upper view, the longitudinal axis of the blade is slightly sigmoidal. A weak and anteriorly directed spur runs diagonally from the cusp. On the lower side, the basal cavity is narrow in the anterior half of the blade and abruptly widens in the posterior half.

Material.—One specimen from sample ALC-13-16m.

Remarks.—The longer and lower blade in our specimen is similar to that of *P. serratus elongatus* Carls and Gandl, 1969. However, in contrast to the latter subspecies, which is distinguished by the distinctly erect denticles in the anterior part and normally two posteriorly reclined cusps in the posterior part, the Alengchu specimen has three proclined denticles at the anterior part of the blade, an undenticulate area in the posterior half of the blade, and one erect cusp. These features readily distinguish this specimen from *P. serratus serratus* Jentzsch, 1962.

Order Protopanderontida Sweet, 1988
Family Protopanderodontidae Lindström, 1970
Genus *Pseudooneotodus* Drygant, 1974

Type species.—*Oneotodus*? *beckmanni* Bischoff and Sannemann, 1958.

Pseudooneotodus beckmanni (Bischoff and Sannemann, 1958)
Figure 5.9

1958 *Oneotodus*? *beckmanni* Bischoff and Sannemann, p. 98, pl. 15, figs. 22–25.
2007 *Pseudooneotodus beckmanni* (Bischoff and Sannemann); Corradini, p. 142, pl. 1, figs. 1–7. [with synonymy list]
2014b *Pseudooneotodus beckmanni* (Bischoff and Sannemann); Corriga et al., fig. 5L.
2014 *Pseudooneotodus beckmanni* (Bischoff and Sannemann); Han et al., pl. 2, figs. 4–10.
2016 *Pseudooneotodus beckmanni* (Bischoff and Sannemann); Corradini et al., pl. 3, fig. 18.
2016 *Pseudooneotodus beckmanni* (Bischoff and Sannemann); Corriga et al., fig. 5S.
2016 *Pseudooneotodus beckmanni* (Bischoff and Sannemann); Mathieson et al., p. 597, fig. 8Q–S. [with synonymy list]
2017 *Pseudooneotodus beckmanni* (Bischoff and Sannemann); Schönlaub et al., pl. 3, fig. 17.
2017 *Pseudooneotodus beckmanni* (Bischoff and Sannemann); Takahashi et al., p. 995, fig. 5.4.
2019 *Pseudooneotodus beckmanni* (Bischoff and Sannemann); Corradini et al., fig. 12S.

Holotype.—Specimen BiSa 1958/85 from the Tentakulitenkalk at Schübelebene near Elbersreuth, Frankenwald, Germany (Bischoff and Sannemann, 1958, pl. 15, fig. 25).

Description.—The short and low conical element has a single apical denticle that is posteriorly reclined. The base of the unit is broad and subtriangular with rounded corners. The lateral surface is distinctly smooth.

https://doi.org/10.1017/jpa.2021.108 Published online by Cambridge University Press

Material.—Five specimens from samples ALC-10-10m (1), ALC-10-19m (2), and ALC-10-23m (2).

Remarks.—The morphological variation of *P. beckmanni* has been extensively studied by Corradini (2007), who also disputed Barrick's (1977) apparatus reconstruction of this species and further suggested, on the basis of material from Sardinia and the Carnic Alps, that this species has a unimembrate apparatus. The broad, subtriangular outline of the base and the single curved tip allow the assignation of our specimens to this species.

Conodont biostratigraphy

In the present study, only 14 samples yielded conodont elements, of which the state of preservation is mostly poor. In general, the abundance is low throughout the lower part of the Shanjiang Formation. All samples from the uppermost part of the underlying Baizitian Formation were completely barren, whereas 64 well-preserved specimens that are assignable to 12 species belonging to 8 genera (*Ancyrodelloides*, *Flajsella*, *Lanea*, *Wurmiella*, *Zieglerodina*, *Caudicriodus*, *Pelekysgnathus*, and *Pseudooneotodus*) were obtained from the lower part of the Shanjiang Formation (Table 1; Fig. 2). Based on the stratigraphic ranges of conodonts, one chronostratigraphic interval (the lower Lochkovian) and one conodont zone (the middle Lochkovian *transitans-pandora* β Zone) are recognized from the lower part of the Shanjiang Formation at the Alengchu section (Fig. 2). The binomial nomenclatural system for time-stratigraphic units described by Murphy (1977) is applied herein to parts of the investigated interval.

The interval ranging from the uppermost part of Bed 9 to the upper part of Bed 10 belongs to the lower Lochkovian. *Caudicriodus* sp. B is recorded in sample ALC-9-10m, which is located ~10 m above the lower boundary of Bed 9, and ranges upwards into sample ALC-10-23m, which is located 23 m above the lower boundary of Bed 10. Three samples were also taken from the lower and middle parts of Bed 9, but only one specimen, assignable to *Wurmiella excavata*, which has been widely documented from the lower Silurian to Lower Devonian, was recovered below the lowest occurrence of *Caudicriodus* sp. B. *Caudicriodus* sp. B shows similarity with *C. hesperius* and *C. woschmidti* in the development of fused transverse ridges on the spindle, a unique feature that is recorded in the early evolution of *Caudicriodus* during the early Lochkovian. As noted earlier, *Caudicriodus* sp. B differs from these two species in the shape of the basal cavity, the outline of the spindle, and/or the length of the posteriorly directed later process. Although the occurrence of *Caudicriodus* sp. B suggests a preliminary correlation of the interval from the uppermost part of Bed 9 to the upper part of Bed 10 with the lower Lochkovian, the precise level of the Silurian-Devonian boundary needs to be investigated further. In addition, other associated fauna includes *Pseudoneotodus beckmanni*, *W. excavata*, *Zieglerodina eladioi*, *Z. planilingua*, and *Z. remscheidensis*; the latter three have their highest occurrences in sample ALC-10-23m.

Lanea omoalpha is recorded at a level 3 m above the base of Bed 11. Its lowest occurrence was previously proposed to define the base of the middle Lochkovian and the base of the *omoalpha-transitans* Zone (Valenzuela-Ríos and Murphy, 1997; Murphy and Valenzuela-Ríos, 1999). As shown by Murphy and Valenzuela-Ríos (1999, text-fig. 1), this taxon ranges from the base of the *omoalpha-transitans* Zone into the *transitans-eleanorae* Zone in Nevada. However, Corradini and Corriga (2012) documented a much lower occurrence of this species in the lower Lochkovian in the Carnic Alps; a similar situation was also encountered in the Prague Synform (Slavík et al., 2012). In order to eliminate the possibility of confusion in the biostratigraphical correlation caused by the range of *L. omoalpha*, Corradini and Corriga (2012) accepted the suggestion of Slavík (2011) and Slavík et al. (2012) that *L. carlsi* (= *Ancyrodelloides carlsi*) acts as a better marker for the lower boundary of the middle Lochkovian. However, Murphy and Valenzuela-Ríos (2017) preferred *A. transitans* to mark the base of the middle Lochkovian because of its distinctive features and wider geographic distribution—a suggestion subsequently supported by Corriga and Corradini (2019b). Accordingly, *L. omoalpha* has a much longer range from the upper part of the *hesperius-carlsi* Zone into the lower part of the *transitans-trigonicus* Zone (Corriga et al., 2014b; Corriga and Corradini, 2019b). Therefore, it is difficult to make a precise biostratigraphical determination for the lower part of Bed 11 with only the single occurrence of *L. omoalpha* in sample ALC-11-3m.

Ancyrodelloides transitans was recorded together with *Wurmiella tuma* in sample ALC-12-6m, which was collected from a level ~6 m above the base of Bed 12. The lowest occurrence of the latter species in sample ALC-11-9m is almost 6 m lower than that of the former one. *Lanea telleri* and *Flajsella stygia* enter together at a slightly higher level, ~10 m above the base of Bed 12. From the overlying strata, only two specimens of *W. tuma* and one specimen of *Pelekysgnathus* sp. A were recovered from the upper part of Bed 13. In contrast to the underlying strata, the interval ranging from sample ALC-11-9m to sample ALC-13-13m contains a distinctly low abundance of conodonts. According to Murphy et al. (2004), *W. tuma* normally has a relatively short stratigraphical range from the upper *eleanorae-trigonicus* Zone to the lower *trigonicus-pandora* β Zone; however, it extends upwards into the *pandora* β-*gilberti* Zone in the Carnic Alps and Sardinia (Corradini and Corriga, 2012, fig. 5). Viewed as the important zonal marker of the *transitans-eleanorae* Zone or *transitans-trigonicus* Zone, *A. transitans* has its lowest occurrence at the base of this zone and its highest occurrence in the *trigonicus-pandora* β Zone (Murphy and Valenzuela-Ríos, 1999, text-fig. 1; Valenzuela-Ríos and Liao, 2012; Valenzuela-Ríos et al., 2015, fig. 4). *Lanea telleri* is restricted to the lower part of the *trigonicus-pandora* β Zone or the *kutscheri-pandora* β Zone in the Spanish Central Pyrenees (Murphy and Valenzuela-Ríos, 1999, text-fig. 4; Valenzuela-Ríos et al., 2015, fig. 4), but it also extends downwards into the *eleanorae-trigonicus* Zone or the upper part of the *transitans-trigonicus* Zone in Nevada (Murphy and Valenzuela-Ríos, 1999, text-fig. 1). In both Nevada and the Spanish Central Pyrenees, *F. stygia* enters in the upper half of the *transitans-trigonicus* Zone (Valenzuela-Ríos and Murphy, 1997, fig. 4; Valenzuela-Ríos and Liao, 2012), and has its highest occurrence in the lower part of the *kutscheri-pandora* β Zone (Valenzuela-Ríos et al., 2015, fig. 4). Additionally, somewhat

https://doi.org/10.1017/jpa.2021.108 Published online by Cambridge University Press

similar ranges of *A. transitans*, *L. telleri*, and *F. stygia* were also observed by Corradini and Corriga (2012, fig. 5) in the Carnic Alps and Sardinia. Taking the stratigraphical ranges of these four species into consideration, it is suggested that the interval from the uppermost part of Bed 11 (sample ALC-11-9m) to the upper part of Bed 13 (sample ALC-13-13m) is correlated with the *transitans-pandora* β Zone. This interval definitely belongs to the middle Lochkovian, the upper limit of which is defined by the entry of *Masarella pandora* β morphotype (Valenzuela-Ríos and Murphy, 1997).

One specimen of *Pelekysgnathus* sp. A was obtained in sample ALC-13-16m from the uppermost part of Bed 13. It differs greatly from previously reported Lochkovian species of this genus. The lack of other important zonal markers in sample ALC-13-16m precludes precise determination of the conodont biostratigraphy for the uppermost part of Bed 13.

Discussion

Wang (1982) first reported the Lochkovian conodont fauna from the Shanjiang Formation or the Lower Devonian at Alengchu and nearby Xiapanluo, which, however, consists of a few specimens of *Caudicriodus woschmidti*, *Spathognathodus remscheidensis*, and *S. wurmi* Bischoff and Sannemann, 1958. Recently, Wang et al. (2018) restudied the Lower Devonian conodont biostratigraphy at the Alengchu section, and roughly defined the bases of the Lochkovian, Pragian, and Emsian. Although few species, of which most have a rather long stratigraphical range and thus are of little biostratigraphical significance, were recorded from the lower part of the Shanjiang Formation, Wang et al. (2018, p. 294) applied the threefold subdivision of the Lochkovian first proposed by Valenzuela-Ríos and Murphy (1997; later modified by Slavík et al., 2012) to the studied succession at the Alengchu section. The lower part of the Lochkovian corresponds to an interval from the base of Bed 9 (also the base of the Shanjiang Formation) to the middle part of Bed 10; the middle part of the Lochkovian starts from the middle part of Bed 10 and ends close to the base of Bed 15; and Bed 15 to Bed 17 were assigned to the upper part of Lochkovian (Wang et al., 2018, fig. 3).

Wang et al. (2018, fig. 6T) obtained only one small icriodontid specimen with three transverse rows of distinct nodes on the short but narrow spindle, a narrow basal cavity, and a well-developed but short posterior lateral process in their sample ALC10-1 from the basal part of Bed 10. They provisionally and equivocally assigned it to *Caudicriodus hesperius*. Taking lithological characters of Bed 9 with respect to the underlying Baizitian Formation and the overlying remaining part of the Shanjiang Formation into consideration, they temporarily located the Silurian-Devonian boundary at the base of the Shanjiang Formation.

In the present study, several adult specimens of *Caudicriodus* sp. B were obtained in a lower level from the uppermost part of Bed 9, which is ~2 m below the level of sample ALC10-1 of Wang et al. (2018). This species shows a close similarity with *C. hesperius* and *C. woschmidti* in the development of the characteristic transverse ridges on the spindle. Moreover, Ma et al. (2017) recognized an intermediate $\delta^{13}C_{carb}$ positive excursion in the basal part of the Shanjiang Formation at the Alengchu section, which indicates that the Silurian-Devonian boundary probably is situated in the basal part of the Shanjiang Formation (Bed 9). It should be noted that, as demonstrated by C.Y. Wang et al. (2009) and Y. Wang et al. (2016), the uppermost Silurian or the Pridoli is probably missing at the Baizitian section, which is also situated in the Panzhihua-Lijiang district. Whether the same situation occurs at the Alengchu needs to be investigated. The entry of *Wurmiella tuma* within the middle part of Bed 9 (third sample ALC9-1c) of H.H. Wang et al. (2018) is noteworthy because this level is slightly higher than the supposed Silurian-Devonian boundary of Wang et al. (2018). *Wurmiella tuma* has a lowest occurrence in the middle Lochkovian *transitans-trigonicus* Zone; thus the reported occurrence by Wang et al. (2018, without illustrations) in such a lower level needs to be examined.

Mainly on the basis of the occurrences of dacryoconarids and the genus *Pandorinellina* Müller and Müller, 1957, Wang et al. (2018, without illustrations) placed the base of the middle part of the Lochkovian roughly in the middle part of Bed 10. As mentioned by Slavík (2011) and Slavík et al. (2012), the phylogenetically oldest dacryoconarids were recorded in the Prague Synform and Carnic Alps within the short range of *Lanea carlsi* (= *Ancyrodelloides carlsi*), whose entry was suggested as a marker of the beginning of the middle Lochkovian. Moreover, the origination of *Pandorinellina* also was demonstrated by Murphy et al. (2004) in the middle Lochkovian. However, our study indicates that the upper part of Bed 10 still belongs to the lower Lochkovian. The reported occurrence of *Pandorinellina* in sample ALC10-4 of Wang et al. (2018) needs to be verified. More importantly, specimens of the zonal marker *A. carlsi* have not been identified at the Alengchu section. Therefore, the accurate position of the lower boundary of the middle Lochkovian is still unknown at this section.

The base of the upper part of the Lochkovian was correlated by Wang et al. (2018) with the base of Bed 15, which is slightly higher than the lowest occurrence of *Masarella pandora* alpha morphotype. Due to the absence of important index taxa from Bed 14 to Bed 17 in the present study, a detailed discussion of the upper Lochkovian is not possible.

Conclusions

The main results of this study on the Lochkovian conodonts at the Alengchu section, western Yunnan is summarized below.

A conodont fauna consisting of 12 taxa assigned to *Ancyrodelloides*, *Flajsella*, *Lanea*, *Wurmiella*, *Zieglerodina*, *Caudicriodus*, *Pelekysgnathus*, and *Pseudooneotodus* was obtained from the lower part (Bed 9 to Bed 13) of the Shanjiang Formation at the Alengchu section. Most of these taxa have been rarely reported in China.

Due to the scarcity of index fossils, the interval ranging from the uppermost part of Bed 9 to the upper part of Bed 10 is assigned roughly to the lower Lochkovian. The Silurian-Devonian boundary is probably located in Bed 9 from the basal part of the Shanjiang Formation.

The interval covering the uppermost part of Bed 11 to the upper part of Bed 13 is correlated with the middle Lochkovian *transitans-pandora* β Zone. This is the first time that the peri-

https://doi.org/10.1017/jpa.2021.108 Published online by Cambridge University Press

Gondwana conodont-based subdivision schemes have been partially tested in China. *Flajsella* and *L. telleri* are documented for the first time in South China.

Acknowledgments

We thank J.I. Valenzuela-Ríos (Valencia) and D.J. Over (Geneseo) for providing important and useful comments that greatly improved the manuscript. T.H. Gao is acknowledged for reading and polishing the manuscript. This work is supported by the Strategic Priority Research Program (B) of the Chinese Academy of Sciences (XDB26000000), the Second Tibetan Plateau Scientific Expedition and Research (No. 2019QZKK0706), the National Natural Science Foundation of China (41872003, 41702009, 91855205), and the Youth Innovation Promotion Association Chinese Academy of Sciences.

References

Barca, S., Gnoli, M., Oliviei, R., and Serpagli, E., 1986, New stratigraphic data and evidence of Lower and Upper Devonian based on conodonts in Sarrabus area (Southeastern Sardinia): Rivista Italiana Di Paleontologia E Stratigrafia, v. 92, p. 299–320.

Bardashev, I.A., 1989, New blade conodonts in the Lower Devonian of central Tadzhikistan, *in* New Species Phanerozoic Fauna and Flora of Tajikistan: Dushanbe, Academy of Sciences of the Tajik SSR, Institute of Geology, Donish, p. 5–14, 211–214. [in Russian]

Bardashev, I.A., and Ziegler, W., 1992, Conodont biostratigraphy of Lower Devonian deposits of the Shishkat section (southern Tien-Shan, Middle Asia): Courier Forschungsinstitut Senckenberg, v. 154, p. 1–29.

Barnett, S.G., 1971, Biometric determination of the evolution of *Spathognathodus remscheidensis*: a method for precise intrabasinal time correlations in the Northern Appalachians: Journal of Paleontology, v. 45, p. 274–300.

Barrick, J.E., 1977, Multielement simple cone conodonts from the Clarita Formation (Silurian), Arbuckle Mountains, Oklahoma: Geologica et Palaeontologica, v. 11, p. 47–68.

Barrick, J.E., and Klapper, G., 1992, Late Silurian–Early Devonian conodonts from the Hunton Group (Upper Henryhouse, Haragan, and Bois d'Arc formations) south-central Oklahoma: Oklahoma Geological Survey Bulletin, v. 145, p. 19–65.

Barrick, J.E., and Noble, P.J., 1995, Early Devonian conodonts from a limestone horizon in the Caballos Novaculite, Marathon Uplift, West Texas: Journal of Paleontology, v. 69, p. 1112–1122.

Barrick, J.E., Meyer, B.D., and Ruppel, S.C., 2005, The Silurian-Devonian boundary and the Klonk event in the Frame Formation, subsurface west Texas: Bulletins of American Paleontology, v. 369, p. 105–122.

Becker, R.T., Marshall, J.E.A., and Da Silva, A.-C., 2020, The Devonian Period, *in* Gradstein, F.M., Ogg, J.G., Schmitz, M.D., and Ogg, G.M., eds., Geological Time Scale 2020: Amsterdam, Elsevier, p. 733–810.

Benfrika, E.M., 1999, Some upper Silurian–Middle Devonian conodonts from the northern part of the Western Meseta of Morocco: systematic and palaeogeographical relationships: Bollettino della Societa Paleontologica Italiana, v. 37, p. 311–320.

Benfrika, E.M., Bultynck, P., and Hassani, A.E., 2007, Upper Silurian to Middle Devonian conodont faunas from the Rabat-Tiflet area (northwestern Moroccan Meseta): Geological Quarterly, v. 51, p. 393–406.

Bischoff, G.C.O., and Argent, J.C., 1990, Lower Devonian (late Lochkovian–Pragian) limestone stratigraphy at [sic] conodont distribution, Waratah Bay, Victoria: Courier Forschungsinstitut Senckenberg, v. 118, p. 441–471.

Bischoff, G., and Sannemann, D., 1958, Unterdevonische conodonten aus dem Frankenwald: Notizblatt des Hessischen Landesamtes für Bodenforschung, v. 86, p. 87–110.

Boersma, K.T., 1973, Description of certain Lower Devonian platform conodonts of the Spanish Central Pyrenees: Leidse Geologische Mededelingen, v. 49, p. 285–301.

Branson, E.B., and Mehl, M.G., 1933, Conodonts from the Bainbridge Formation (Silurian) of Missouri: University of Missouri Studies, v. 8, p. 39–52.

Bultynck, P., 1976, Le Silurien Supérieur et le Devonien Inferieur de la Sierra de Guadarrama (Espagne Centrale). Troisiéme partie: elements Icriodiformes, Pelekysgnathiformes et Polygnathiformes: Bulletin de l' Institut royal des Sciences naturalles de Belgique, Sciences de la Terre, v. 49, p. 1–74.

Carls, P., 1975, Zusätzliche Conodonten-Funde aus dem tieferen Unter-Devon Keltiberiens (Spanien): Senckenbergiana Lethaea, v. 56, p. 399–428.

Carls, P., and Gandl, J., 1969, Stratigraphie und conodonten des Unter-Devons der Östlichen Iberischen Ketten (NE-Spanien): Neues Jahrbuch für Geologie und Paläontologie Abhandlungen, v. 132, p. 155–218.

Chatterton, B.D.E., and Perry, D.G., 1977, Lochkovian trilobites and conodonts from northwestern Canada: Journal of Paleontology, v. 51, p. 772–796.

Chen, Z.Y., Männik, P., Wang, C.Y., Fang, X., Chen, T.E., Ma, X., and Zhang, Y.D., 2020, Silurian conodont biostratigraphy of the Laojianshan section, Baoshan, Yunnan Province, SW China: Geological Journal, v. 55, p. 6427–6441.

Chlupáč, I., Kriz, J., and Schönlaub, H.P., 1980, Field Trip E: Silurian and Devonian conodont localities of the Barrandian, *in* Schönlaub, H.P., ed., Second European Conodont Symposium (ECOS II), Guidebook, Abstracts: Abhandlungen der Geologischen Bundesanstalt, v. 35, p. 147–180.

Clark, D.L., and Ethington, R.L., 1966, Conodonts and biostratigraphy of the Lower and Middle Devonian of Nevada and Utah: Journal of Paleontology, v. 40, p. 659–689.

Colquhoun, G.P., 1995, Early Devonian conodont faunas from the Capertee High, NE Lachlan Fold Belt, southeastern Australia: Courier Forschungsinstitut Senckenberg, v. 182, p. 347–369.

Corradini, C., 2007, The conodont genus *Pseudooneotodus* Drygant from the Silurian and Lower Devonian of Sardinia and the Carnic Alps (Italy): Bollettino della Societa Paleontologica Italiana, v. 46, p. 139–148.

Corradini, C., and Corriga, M.G., 2010, Silurian and lowermost Devonian conodonts from the Passo Volaia area (Carnic Alps, Italy): Bollettino della Societa Paleontologica Italiana, v. 49, p. 237–253.

Corradini, C., and Corriga, M.G., 2012, A Přídolí–Lochkovian conodont zonation in Sardinia and the Carnic Alps: implications for a global zonation scheme: Bulletin of Geosciences, v. 87, p. 635–650.

Corradini, C., Leone, F., Loi, A., and Serpagli, E., 2001, Conodont stratigraphy of a highly tectonised Silurian–Devonian section in the San Basilio area (SE Sardinia, Italy): Bollettino della Società Paleontologica Italiana, v. 40, p. 315–323.

Corradini, C., Simonetto, L., Serventi, P., Rigo, R., and Calligaris, C., 2005, Loboliti (Crinoidea) del Devoniano basale di Monte Zermula (Alpi Carniche Italiane): Rendiconti della Società Paleontologica Italiana, v. 2, p. 29–36.

Corradini, C., Pondrelli, M., Simonetto, L., Corriga, M.G., Spaletta, C., Suttner, T.J., Kido, E., Mossoni, A., and Serventi, P., 2016, Stratigraphy of the La Valute area (Mt. Zermula massif, Carnic Alps, Italy): Bollettino della Societa Paleontologica Italiana, v. 55, p. 55–78.

Corradini, C., Corriga, M.G., Pondrelli, M., Serventi, P., Simonetto, L., and Ferretti, A., 2019, Lochkovian (Lower Devonian) marine-deposits from the Rio Malinfier West section (Carnic Alps, Italy): Italian Journal of Geosciences, v. 138, p. 153–170.

Corradini, C., Corriga, M.G., Pondrelli, M., and Suttner, T.J., 2020, Conodonts across the Silurian/Devonian boundary in the Carnic Alps (Austria and Italy): Palaeogeography, Palaeoclimatology, Palaeoecology, v. 549, 109097. https://doi.org/10.1016/j.palaeo.2019.02.023.

Corriga, M.G., and Corradini, C., 2009, Upper Silurian and Lower Devonian conodonts from the Monte Cocco II Section (Carnic Alps, Italy): Bulletin of Geosciences, v. 84, p. 155–168.

Corriga, M.G., and Corradini, C., 2019a, The conodont apparatus of *Zieglerodina eladioi* (Valenzuela-Ríos, 1994): Bollettino della Societa Paleontologica Italiana, v. 58, p. 181–185.

Corriga, M.G., and Corradini, C., 2019b, Ontogeny of *Ancyrodelloides carlsi* (Boersma) and comments on its generic attribution (Conodonta, Lower Devonian): Geobios, v. 57, p. 25–32.

Corriga, M. G., Corradini, C., Haude, R., and Walliser, O.H., 2014a, Conodont and crinoid stratigraphy of the upper Silurian and Lower Devonian scyphocrinoid beds of Tafilalt, southeastern Morocco: GFF, v. 136, p. 65–69.

Corriga, M. G., Corradini, C., and Walliser, O.H., 2014b, Upper Silurian and Lower Devonian conodonts from Tafilalt, southeastern Morocco: Bulletin of Geosciences, v. 89, p. 183–200.

Corriga, M.G., Corradini, C., Schönlaub, H.P., and Pondrelli, M., 2016, Lower Lochkovian (Lower Devonian) conodonts from Cellon section (Carnic Alps, Austria): Bulletin of Geosciences, v. 91, p. 261–270.

Druce, E.C., 1970, Lower Devonian conodonts from the northern Yarrol Basin, Queensland: Australian Bureau of Mineral Resources, Geology and Geophysics Bulletin, v. 108, p. 43–73.

Drygant, D.M., 1974, Prostye konodonty silura i nizov devona Volyno-Podol'ya: Palaeontologicheskii Sbornik, v. 10, p. 64–70. [in Russian]

Drygant, D.M., 1984, Korrelacia i konodonty silurijskih–nižniedevonskih otloženij Volyno–Podolii: Kiyev, Naukova Dumka, 192 p. [in Russian]

Drygant, D., and Szaniawski, H., 2012, Lochkovian conodonts from Podolia, Ukraine, and their stratigraphic significance: Acta Palaeontologica Polonica, v. 57, p. 833–861.

Dzik, J., 1976, Remarks on the evolution of Ordovician conodonts: Acta Palaeontologica Polonica, v. 21, p. 395–455.
Fåhræus, L.E., 1969, Conodont zones in the Ludlovian of Gotland and a correlation with Great Britain: Sveriges Geologiska Undersökning Ser. C, v. 63, p. 1–33.
Fåhræus, L.E., 1971, Lower Devonian conodonts from the Michelle and Prongs Creek formations, Yukon Territory: Journal of Paleontology, v. 45, p. 665–683.
Farrell, J.R., 2003, Late Pridolian, Lochkovian, and early Pragian conodonts from the Gap area between Larras Lee and Eurimbla, central western NSW, Australia: Courier Forschungsinstitut Senckenberg, v. 245, p. 107–181.
Farrell, J.R., 2004, Siluro-Devonian conodonts from the Camelford Limestone, Wellington, New South Wales, Australia: Palaeontology, v. 47, p. 937–982.
Flajs, G., 1966, Conodontenstratigraphische untersuchungen im Raum von Eisenerz, Nördliche Grauwackenzone: Mitteilungen der Geologischen Gesellschaft in Wien, v. 59, p. 157–212.
Gaetani, M., Mawson, R., Sciunnach, D., and Talent, J., 2008, The Devonian of Western Karakorum (Pakistan): Acta Geologica Polonica, v. 58, p. 261–285.
García-López, S., Sanz-López, J., and Sarmiento, G.N., 2002, Uppermost Pridoli to upper Emsian stratigraphy of the Alto Carrión unit, Palentine Domain (Northwest Spain), *in* García-López, S., and Bastida, F., eds., Palaeozoic Conodonts from Northern Spain: Cuadernos del Museo Geominero, v. 1, p. 125–161.
Han, C.Y., Zhang, F., Wang, C.Y., Wu, J., and Hou, F.M., 2014, Age of the Niqiuhe Formation in Sunitezuo Qi, Inner Mongolia based on conodonts: Acta Micropalaeontologica Sinica, v. 31, p. 257–270. [in Chinese with English abstract]
Hass, W.H., 1959, Conodonts from the Chappel Limestone of Texas: United States Geological Survey Professional Paper 294J, p. 365–400.
Hušková, A., and Slavík, L., 2020, In search of Silurian/Devonian boundary conodont markers in carbonate environments of the Prague Synform (Czech Republic): Palaeogeography, Palaeoclimatology, Palaeoecology, v. 549, 109126. https://doi.org/10.1016/j.palaeo.2019.03.027.
Jansen, U., Lazreq, N., Plodowski, G., Schemm-Gregory, M., Schindler, E., and Weddige, K., 2007, Neritic-pelagic correlation in the Lower and basal Middle Devonian of the Dra Valley (southern Anti-Atlas, Moroccan pre-Sahara), *in* Becker, R.T., and Kirchgasser, W.T., eds., Devonian Events and Correlations: Geological Society, London, Special Publications, v. 278, p. 9–37.
Jentzsch, I., 1962, Conodonten aus dem tentaculitenknollenkalk (Unterdevon) in Thüringen: Geologie, v. 11, p. 961–985.
Jeppsson, L., 1989, Latest Silurian conodonts from Klonk, Czechoslovakia: Geologica et Palaeontologica, v. 23, p. 21–37.
Jiang, Z.W., 1980, Early Lower Devonian tentaculites from western Yunnan: Acta Palaeontologica Sinica, v. 19, p. 505–510. [in Chinese with English abstract]
Jin, C.T., Qian, Y.Z., and Wang, J.L., 2005, Silurian conodont succession and chronostratigraphy of the Baizitian region in Yanbian, Panzhihua, Sichuan: Journal of Stratigraphy, v. 29, p. 281–294. [in Chinese with English abstract]
Klapper, G., 1977, Lower and Middle Devonian conodont sequence in central Nevada, *in* Murphy, M.A., Berry, W.B.N., and Sandberg, C.A., eds., Western North America Devonian: University of California, Riverside, Campus Museum Contribution, v. 4, p. 33–54.
Klapper, G., and Johnson, J.G., 1980, Endemism and dispersal of Devonian conodonts: Journal of Paleontology, v. 54, p. 400–455.
Klapper, G., and Murphy, M.A., 1975, Silurian–Lower Devonian conodont sequence in the Roberts Mountains Formation of central Nevada: University of California Publications in Geological Sciences, v. 111, p. 1–62. [imprint 1974]
Kuwano, Y., 1987, Early Devonian conodonts and ostracodes from central Japan: Bulletin of the National Science Museum, Series C, Geology & Palaeontology, v. 13, p. 77–105.
Lane, H.R., and Ormiston, A.R., 1979, Siluro-Devonian Biostratigraphy of the Salmontrout River area, east-central Alaska: Geologica et Palaeontologica, v. 13, p. 39–96.
Lazreq, N. and Ouanaimi, H., 1998, Le Dévonien inférieur de Tizi-n-Tichka (Haut Atlas) et de Laàyoune (Tata, Anti-Atlas, Maroc): nouvelles datations et implications paléogéographiques: Senckenbergiana Lethaea, v. 77, p. 223–231.
Li, J.S., 1987, Late Silurian–Devonian conodonts from Luqu-Tewo region, West Qinling Mts., China, *in* Xi'an Institute of Geology and Mineral Resources, and Nanjing Institute of Geology and Palaeontology, Academia Sinica, eds., Late Silurian–Devonian Strata and Fossils from Luqu-Tewo Area of West Qinling Mountains, China, Volume 2: Nanjing, Nanjing University Press, p. 357–378. [in Chinese with English abstract]
Liao, W.H., and Xia, F.S., 1996, Geological age of Arpishmebulaq Formation in eastern part of South Tianshan Mountains, Xinjiang: Xinjiang Petroleum Geology, v. 17, p. 138–144. [in Chinese with English abstract]
Lindström, M., 1970, A suprageneric taxonomy of the conodonts: Lethaia, v. 3, p. 427–445.
Link, A.G., and Druce, E.C., 1972, Ludlovian and Gedinnian conodont stratigraphy of the Yass Basin, New South Wales: Australian Bureau of Mineral Resources, Geology and Geophysics Bulletin, v. 134, p. 1–136.
Lu, J.F., and Chen, X.Q., 2016, New insights into the base of the Emsian (Lower Devonian) in South China: Geobios, v. 49, p. 459–467.
Ma, X.P., Wang, H.H., and Zhang, M.Q., 2017, Devonian event succession and sea level change in South China—with Early and Middle Devonian carbon and oxygen isotopic data: Subcommission on Devonian Stratigraphy Newsletter, v. 32, p. 17–24.
Mashkova, T.V., 1972, *Ozarkodina steinhornensis* (Ziegler) apparatus, its conodonts and biozone: Geologica et Palaeontologica, v. SB1, p. 81–90.
Mastandrea, A., 1985a, Early Devonian (Lochkovian) conodonts from southwestern Sardinia, Bollettino della Società Paleontologica Italiana, v. 23, p. 240–258.
Mastandrea, A., 1985b, Biostratigraphic remarks on early Devonian conodonts from Corti Baccas III section (SW Sardinia): Bollettino della Societa Paleontologica Italiana, v. 23, p. 259–267.
Mathieson, D., Mawson, R., Simpson, A.J., and Talent, J.A., 2016, Late Silurian (Ludlow) and Early Devonian (Pragian) conodonts from the Cobar Supergroup, western New South Wales, Australia: Bulletin of Geosciences, v. 91, p. 583–652.
Mavrinskaya, T., and Slavík, L., 2013, Correlation of Early Devonian (Lochkovian–early Pragian) conodont faunas of the South Urals (Russia): Bulletin of Geosciences, v. 88, p. 283–296.
Mawson, R., 1986, Early Devonian (Lochkovian) conodont faunas from Windellama, New South Wales: Geologica et Palaeontologica, v. 20, p. 39–71.
Mawson, R., and Talent, J.A., 1994, Age of an Early Devonian carbonate fan and isolated limestone clasts and megaclasts, east-central Victoria: Proceedings of the Royal Society of Victoria, v. 106, p. 31–70.
Mawson, R., Talent, J.A., Molloy, P.D., and Simpson, A.J., 2003, Siluro-Devonian (Pridoli–Lochkovian and early Emsian) conodonts from the Nowshera area, Pakistan: implications for the mid-Palaeozoic stratigraphy of the Peshawar Basin: Courier Forschungsinstitut Senckenberg, v. 245, p. 83–105.
Medici, L., Malferrari, D., Savioli, M., and Ferretti, A., 2020, Mineralogy and crystallization patterns in conodont bioapatite from first occurrence (Cambrian) to extinction (end-Triassic): Palaeogeography, Palaeoclimatology, Palaeoecology, v. 549, 109098. https://doi.org/10.1016/j.palaeo.2019.02.024.
Mehrtens, C.J., and Barnett, S.G., 1976, Conodont subspecies from the upper Silurian–Lower Devonian of Czechoslovakia: Micropaleontology, v. 22, p. 491–500.
Miller, C.G., and Aldridge, R.J., 1997, *Ozarkodina remscheidensis* plexus conodonts from the upper Ludlow (Silurian) of the Welsh Borderland and Wales: Journal of Micropalaeontology, v. 16, p. 41–49.
Müller, K.J., and Müller, E.M., 1957, Early Upper Devonian (Independence) conodonts from Iowa, part I: Journal of Paleontology, v. 31, p. 1069–1108.
Murphy, M.A., 1977, On time-stratigraphic units: Journal of Paleontology, v. 51, p. 213–219.
Murphy, M.A., 2016, *Cypricriodus hesperius* (Klapper and Murphy, 1975) taxonomy and biostratigraphy: University of California, Riverside Campus Museum Contribution, v. 8, p. 1–24.
Murphy, M.A., and Cebecioglu, M.K., 1986, Statistical study of *Ozarkodina excavata* (Branson and Mehl) and *O. tuma* Murphy and Matti (Lower Devonian, *delta* Zone, conodonts, Nevada): Journal of Paleontology, v. 60, p. 865–869.
Murphy, M.A., and Matti, J.C., 1983, Lower Devonian conodonts (*hesperius–kindlei* zones), central Nevada: University of California Publications in Geological Sciences, v. 123, p. 1–83. [imprint 1982]
Murphy, M.A., and Valenzuela-Ríos, J.I., 1999, *Lanea* new genus, lineage of Early Devonian conodonts: Bollettino della Societa Paleontologica Italiana, v. 37, p. 321–334.
Murphy, M.A. and Valenzuela-Ríos, J.I., 2017, Reconstruction of the skeletal apparatus of *Flajsella* Valenzuela-Rios and Murphy 1997 (Devonian conodont): Stratigraphy, v. 14, p. 285–297.
Murphy, M.A., Matti, J.C., and Walliser, O.H., 1981, Biostratigraphy and evolution of the *Ozarkodina remscheidensis-Eognathodus sulcatus* lineage (Lower Devonian) in Germany and central Nevada: Journal of Paleontology, v. 55, p. 747–772.
Murphy, M.A., Valenzuela-Ríos, J.I., and Carls, P., 2004, On classification of Pridoli (Silurian)–Lochkovian (Devonian) Spathognathodontidae (conodonts): University of California, Riverside, Campus Museum Contributions, v. 6, p. 1–25.
Olivieri, R., and Serpagli, E., 1990, Latest Silurian–Early Devonian conodonts from the Mason Porcus section near Fluminimaggiore, Southwestern Sardinia: Bollettino della Societa Paleontologica Italiana, v. 29, p. 59–76.

https://doi.org/10.1017/jpa.2021.108 Published online by Cambridge University Press

Pickett, J., 1980, Conodont assemblages from the Cobar Supergroup (Early Devonian), New South Wales: Alcheringa, v. 4, p. 67–88.
Rexroad, C.B., and Craig, W.W., 1971, Restudy of Conodonts from the Bainbridge Formation (Silurian) at Lithium, Missouri: Journal of Paleontology, v. 45, p. 684–703.
Rong, J.Y, Chen, X., Su, Y.Z., Ni, Y.N., Zhan, R.B., Chen, T.E., Fu, L.P., Li, R.Y., and Fan, J.X., 2003, Silurian paleogeography of China: New York State Museum Bulletin, v. 493, p. 243–298.
Sanz-López, J., Perret, M.-F., and Vachard, D., 2006, Silurian to Mississippian series of the eastern Catalan Pyrenees (Spain), updated by conodonts, foraminifers and algae: Geobios, v. 39, p. 709–725.
Savage, N.M., 1973, Lower Devonian conodonts from New South Wales: Palaeontology, v. 16, p. 307–333.
Savage, N.M., 1982, Lower Devonian (Lochkovian) conodonts from Lulu Island, southeastern Alaska: Journal of Paleontology, v. 56, p. 983–988.
Schönlaub, H.P., 1980, Field trip A: Carnic Alps, *in* Schönlaub, H.P., ed., Second European Conodont Symposium (ECOS II), Guidebook, Abstracts: Abhandlungen der Geologischen Bundesanstalt, v. 35, p. 5–59.
Schönlaub, H.P., 1985, Devonian conodonts from section Oberbuchach II in the Carnic Alps (Austria): Courier Forschungsinstitut Senckenberg, v. 75, p. 353–374.
Schönlaub, H. P., Corradini, C., Corriga, M.G., and Ferretti, A., 2017, Chrono-, litho- and conodont bio-stratigraphy of the Rauchkofel Boden section (Upper Ordovician–Lower Devonian), Carnic Alps, Austria: Newsletters on Stratigraphy, v. 50, p. 445–469.
Schulze, R., 1968, Die Conodonten aus dem Palaeozoikum der mittleren Karawanken (Seeberggebiet): Neues Jahrbuch für Geologie und Paläontologie Abhandlungen, v. 130, p. 133–240.
Serpagli, E., and Mastandrea, A., 1980, Conodont assemblages from the Silurian-Devonian boundary beds of southwestern Sardinia (Italy): Neues Jahrbuch fur Geologie und Palaontologie Monatshefte, v. 1, p. 37–42.
Serpagli, E., Gnoli, M., Mastandrea, A., and Olivieri, R., 1978, Palaeontological evidence of the Gedinnian (Lower Devonian) in southwestern Sardinia: Rivista Italiana Di Paleontologia e Stratigrafia, v. 84, p. 305–312.
Slavík, L., 1998, Early Devonian conodont succession from the section of the Čertovy Schody Quarry (Koněprusy, Barrandian, Czech Republic): Věstnik Českého Geologického Ústavu, v. 73, p. 157–172.
Slavík, L., 2011, *Lanea carlsi* conodont apparatus reconstruction and its significance for subdivision of the Lochkovian: Acta Palaeontologica Polonica, v. 56, p. 313–327.
Slavík, L., 2017, Conodonts from the Silurian and Devonian of the Požáry Quarries, *in* Suttner, T.J., Valenzuela-Ríos, J.I., Liao, J.-C., Corradini, C., and Slavík, L., eds., International Conodont Symposium 4: Progress on Conodont Investigation, Valencia 25–30th June 2017, Field Guide Book: Berichte des Institutes für Erdwissenschaften, Karl-Franzens-Universität Graz, v. 23., p. 139–152.
Slavík, L., Carls, P., Hladil, J., and Koptíková, L., 2012, Subdivision of the Lochkovian Stage based on conodont faunas from the stratotype area (Prague Synform, Czech Republic): Geological Journal, v. 47, p. 616–631.
Sloan, T.R., Talent, J.A., Mawson, R., Simpson, A.J., Brock, G.A., Engelbretsen, M.J., Jell, J.S., Aung, A.K, Pfaffenritter, C., Trotter, J., and Withnall, I.W., 1995, Conodont data from Silurian–Middle Devonian carbonate fans, debris flows, allochthonous blocks and adjacent autochthonous platform margins: Broken River and Camel Creek areas, North Queensland, Australia: Courier Forschungsinstitut Senckenberg, v. 182, p. 1–77.
Sorentino, L., 1989, Conodont assemblages spanning the Lochkovian-Pragian (Early Devonian) boundary at Eurimbla, central New South Wales: Courier Forschungsinstitut Senckenberg, v. 117, p. 81–115.
Suttner, T.J., 2007, Conodont stratigraphy, facies-related distribution patterns and stable isotopes (carbon and oxygen) of the uppermost Silurian to Lower Devonian Seewarte section (Carnic Alps, Carinthia, Austria): Abhandlungen der Geologischen Bundesanstalt, v. 59, p. 1–111.
Suttner, T.J., 2009, Lower Devonian conodonts of the "Baron von Kottwitz" quarry (Southern Burgenland, Austria), *in* Over, D.J., ed., Conodont Studies Commemorating the 150th Anniversary of the First Conodont Paper (Pander, 1856) and the 40th Anniversary of the Pander Society: Palaeontographica Americana, v. 62, p. 75–87.
Sweet, W.C., 1988, The Conodonta: Morphology, Taxonomy, Paleoecology, and Evolutionary History of a Long-Extinct Animal Phylum: Oxford, Oxford Monographs on Geology and Geophysics, No. 10, 212 p.
Takahashi, Y., Agematsu, S., Rahman, M.N.A., and Sashida, K., 2017, Lowermost Devonian conodonts from the Setul Group, northwestern Peninsular Malaysia: The Journal of the Geological Society of Japan, v. 123, p. 989–997.
Talent, J.A., and Mawson, R., 1999, North-eastern Molong Arch and adjacent Hill End Trough (eastern Australia): mid-Palaeozoic conodont data and implication: Abhandlungen der Geologischen Bundesanstalt, v. 54, p. 49–105.
Thomas, L.A., 1949, Devonian–Mississippian formations of southeast Iowa: Geological Society of America Bulletin, v. 60, p. 403–438.
Trotter, J.A., and Talent, J.A., 2005, Early Devonian (mid-Lochkovian) brachiopod, coral and conodont faunas from Manildra, New South Wales, Australia: Palaeontographica A, v. 273, p. 1–54.
Uyeno, T.T., 1980, Part II: systematic study of conodonts, *in* Thorsteinsson, R., and Uyeno, T.T., eds., Stratigraphy and Conodonts of Upper Silurian and Lower Devonian Rocks in the Environs of the Boothia Uplift, Canadian Arctic Archipelago: Geological Survey of Canada Bulletin, v. 292, p. 39–75.
Uyeno, T.T., 1990, Biostratigraphy and conodont faunas of Upper Ordovician through Middle Devonian rocks, eastern Arctic Archipelago: Geological Survey of Canada Bulletin, v. 401, p. 1–211.
Uyeno, T.T., 1991, Pre-Famennian Devonian conodont biostratigraphy of selected intervals in the eastern Canadian Cordillera: Geological Survey of Canada Bulletin, v. 417, p. 129–161.
Valenzuela-Ríos, J.I., 1994a, Conodontos del Lochkoviense y Praguiense (Devónico Inferior) del Pirineo Central Español: Memorias del Museo Paleontológico de la Universidad de Zaragoza, v. 5, 178 p.
Valenzuela-Ríos, J.I., 1994b, The Lower Devonian conodont *Pedavis pesavis* and the *pesavis* Zone: Lethaia, v. 27, p. 199–207.
Valenzuela-Ríos, J.I., 2002, Lochkovian and Pragian Conodonts from Segre 1 (Central Spanish Pyrenees), *in* García-López, S., and Bastida, F., eds., Palaeozoic Conodonts from Northern Spain: Cuadernos del Museo Geominero, v. 1, p. 403–417.
Valenzuela-Ríos, J.I., and García-López, S., 1998, Using conodonts to correlate abiotic events: an example from the Lochkovian (Early Devonian) of NE Spain: Palaeontologia Polonica, v. 58, p. 191–199.
Valenzuela-Ríos, J.I., and Liao, J.-C., 2012, Color/Facies changes and global events, a hoax? A case study from the Lochkovian (Lower Devonian) in the Spanish Central Pyrenees: Palaeogeography, Palaeoclimatology, Palaeoecology, v. 367–368, p. 219–230.
Valenzuela-Ríos, J.I., and Liao, J.-C., 2017, Middle and upper Lochkovian (Lower Devonian) at Segre 5 section, *in* Suttner, T.J., Valenzuela-Ríos, J.I., Liao, J.-C., Corradini, C., and Slavík, L., eds., International Conodont Symposium 4: Progress on Conodont Investigation, Valencia 25–30th June 2017, Field Guide Book: Berichte des Institutes für Erdwissenschaften, Karl-Franzens-Universität Graz, v. 23., p. 65–67.
Valenzuela-Ríos, J.I., and Murphy, M.A., 1997, A new zonation of middle Lochkovian (Lower Devonian) conodonts and evolution of *Flajsella* n. gen. (Conodonta), *in* Klapper, G., Murphy, M.A., and Talent, J.A., eds., Paleozoic Sequence Stratigraphy, Biostratigraphy, and Biogeography: Studies in Honor of J. Granville ("Jess") Johnson: Geological Society of America Special Paper, v. 321, p. 131–144.
Valenzuela-Ríos, J.I., Liao, J.-C., Martínez-Pérez, C., Castelló, V., and Botella, H., 2005, Datos preliminares sobre los conodontos y restos de peces del Lochkoviense (Devónico Inferior) de Compte-I (Valle del Noguera Pallaresa, Pirineos), *in* Gámez, J.A., Liñán, E., and Valenzuela-Ríos, J.I., eds., Memorias de las VIII Jornadas Aragonesas de Paleontología: "La cooperación Internacional en la Paleontología Española. Homenaje al Profesor Peter Carls": Zaragoza, Institución "Fernando el Católico", p. 131–145.
Valenzuela-Ríos, J.I., Slavík, L., Liao, J.-C., Calvo, H., Hušková, A., Chadimová, L., 2015, The middle and upper Lochkovian (Lower Devonian) conodont successions in key peri-Gondwana localities (Spanish Central Pyrenees and Prague Synform) and their relevance for global correlations: Terra Nova, v. 27, p. 409–415.
Valenzuela-Ríos, J.I., Liao, J.-C., and Martínez-Pérez, C., 2017a, Lochkovian and Pragian (Lower Devonian) at Segre 1–2 sections, *in* Suttner, T.J., Valenzuela-Ríos, J.I., Liao, J.-C., Corradini, C., and Slavík, L., eds., International Conodont Symposium 4: Progress on Conodont Investigation, Valencia 25–30th June 2017, Field Guide Book: Berichte des Institutes für Erdwissenschaften, Karl-Franzens-Universität Graz, v. 23., p. 53–60.
Valenzuela-Ríos, J.I., Liao, J.-C., and Calvo, H., 2017b, Middle and upper Lochkovian (Lower Devonian) at Segre 4 section, *in* Suttner, T.J., Valenzuela-Ríos, J.I., Liao, J.-C., Corradini, C., and Slavík, L., eds., International Conodont Symposium 4: Progress on Conodont Investigation, Valencia 25–30th June 2017, Field Guide Book: Berichte des Institutes für Erdwissenschaften, Karl-Franzens-Universität Graz, v. 23., p. 61–64.
Walliser, O.H., 1964, Conodonten des Silurs: Abhandlungen des Hessischen Landesamtes für Bodenforschung, v. 41, p. 1–106.
Wang, B.Y., Zhang, Z.X., Rong, J.Y., Wang, C.Y., and Cai, T.C., 2001, Silurian and Early Devonian Stratigraphy and Faunas in Southern Tianshan, Xinjiang: Hefei, University of Science and Technology of China Press, 130 p. [in Chinese]
Wang, C.Y., 1979, Some conodonts from the Sipai Formation in Xianzhou of Guangxi: Acta Palaeontologica Sinica, v. 18, p. 395–407. [in Chinese with English abstract]
Wang, C.Y., 1981, Lower Devonian conodonts from the Xiaputonggou Formation at Zoige, NW Sichuan: Bulletin of the Xi'an Institute of Geology and Mineral Resources, Chinese Academy of Geological Sciences, v. 3, p. 76–84. [in Chinese with English abstract]

https://doi.org/10.1017/jpa.2021.108 Published online by Cambridge University Press

Wang, C.Y., 1982, Upper Silurian and Lower Devonian conodonts from Lijiang of Yunnan: Acta Palaeontologica Sinica, v. 21, p. 436–448. [in Chinese with English abstract]
Wang, C.Y., 1983, Silurian and Lower Devonian conodonts from Darhan Mumingan Joint Banner, Inner Mongolia, *in* Li, W.G., Rong, J.Y., and Dong, D.Y., eds., Silurian and Devonian Rocks and Faunas of the Bateaobao Area in Darhan Mumingan Joint Banner, Inner Mongolia: Hohhot, The People's Publishing House of Inner Mongolia, p. 153–164. [in Chinese with English abstract]
Wang, C.Y., and Zhang, S.A., 1988, Discovery of the early Early Devonian conodonts from the Kuche area of Xinjiang: Journal of Stratigraphy, v. 12, p. 147–150. [in Chinese]
Wang, C.Y., and Ziegler, W., 1983, Conodonts from Tibet: Neues Jahrbuch für Geologie und Paläontologie Monatshefte, v. 1983, p. 69–79.
Wang, C.Y., Zhou, M.K., Yan, Y.J., Wu, Y.L., Zhao, Y.G., and Qian, Y.Z., 2000, Lower Devonian conodonts from the Sawayardun Goldmine area, Wuqia (Ulugqat) County, Xinjiang: Acta Micropalaeontologica Sinica, v. 17, p. 255–264. [in Chinese with English abstract]
Wang, C.Y., Weddige, K., Ziegler, W., and Minjin, C., 2005a, New record of Devonian Lochkovian conodonts from the Tsagaanbulag Formation in the Shine Jinst area, South Mongolia: Acta Palaeontologica Sinica, v. 44, p. 17–24.
Wang, C.Y., Minjin, C., Ziegler, W., Munchtsetseg, J., Gereltsetseg, J., and Undarya, J., 2005b, The first discovery of the middle Lochkovian (Devonian) conodonts in South Gobi, Mongolia: Science in China Series D: Earth Sciences, v. 48, p. 48–52.
Wang, C.Y., Wang, P., Yang, G.H., and Xie, W., 2009, Restudy of the Silurian conodont biostratigraphy of the Baizitian section in Yanbian County, Sichuan: Journal of Stratigraphy, v. 33, p. 302–317. [in Chinese with English abstract]
Wang, H.H., Ma, X.P., Slavík, L., Wei, F., Zhang, M.Q., and Lü, D., 2018, Lower Devonian conodont biostratigraphy of the Alengchu section in Western Yunnan Province, South China: Journal of Stratigraphy, v. 42, p. 288–300. [in Chinese with English abstract]
Wang, P., 2006, Lower Devonian conodonts of the Bateaobao area in Darhan Muming'an Joint Banner, Inner Mongolia: Acta Micropalaeontologica Sinica, v. 23, p. 199–234. [in Chinese with English summary]
Wang, Y., Rong, J.Y., Tang, P., Wang, G.X., and Zhang, X.L., 2016, New observation on the Silurian Baizitian section from Yanbian, Western Sichuan, SW China: Journal of Stratigraphy, v. 40, p. 225–233. [in Chinese with English abstract]
Weyant, M., and Morzadec, P., 1990, Datation par les conodontes de la partie Supérieure de la formation de Gahard (Dévonien Inféieur) à Sablé-sur-Sarthe (est du Massif Armorican): Geobios, v. 23, p. 749–754.
Wilson, G.A., 1989, Documentation of conodont assemblages across the Lochkovian-Pragian (Early Devonian) boundary at Wellington, central New South Wales, Australia: Courier Forschungsinstitut Senckenberg, v. 117, p. 117–171.
Xia, F.S., 1997, Conodonts from the Arpishmebulaq Formation (late Lochkovian) of eastern south Tianshan and their significance: Acta Palaeontologica Sinica, v. 36, p. 77–103. [in Chinese with English summary]
Yu, C.M., and Liao, W.H., 1978, Lower Devonian rugose corals from Alengchu of Lijiang, northwestern Yunnan: Acta Palaeontologica Sinica, v. 17, p. 245–266. [in Chinese with English abstract]
Zhang, G.W., Guo, A.L., Wang, Y.J., Li, S.Z., Dong, Y.P., Liu, S.F., He, D.F., Chen, S.Y., Lu, R.K., and Yao, A.P., 2013, Tectonics of South China continent and its implications: Science China: Earth Sciences, v. 56, p. 1804–1828.
Zhen, Y.Y., Hegarty, R., Percival, I.G., and Pickett, J.W., 2017, Early Devonian conodonts from the southern Thomson Orogen and northern Lachlan Orogen in north-western New South Wales: Proceedings of the Linnean Society of New South Wales, v. 139, p. 69–83.
Ziegler, W., 1960, Conodonten aus dem Rheinischen Unterdevon (Gedinnium) des Remscheider Sattels (Rheinisches Schiefergebirge): Paläontologische Zeitschrift, v. 34, p. 169–201.
Ziegler, W., ed., 1991, Catalogue of Conodonts, Volume V: Stuttgart, E. Schweizerbart'sche Verlagsbuchhandlung, 212 p.

Accepted: 22 October 2021